Emergency Delivery of Vasopressin from an Implantable MEMS Rapid Drug Delivery Device

by

Hong Linh Ho Duc

B.S./M.S. Materials Engineering
Drexel University, 2002

S.M. Materials Science & Engineering
Massachusetts Institute of Technology, 2005

SUBMITTED TO THE DEPARTMENT OF MATERIALS SCIENCE & ENGINEERING IN PARTIAL FULFILLMENT OF THE REQUIREMENTS FOR THE DEGREE OF

DOCTOR OF PHILOSOPHY IN MATERIALS SCIENCE & ENGINEERING
AT THE
MASSACHUSETTS INSTITUTE OF TECHNOLOGY

JUNE 2009

Signature of Author: _____
Department of Materials Science & Engineering
May 6, 2009

Certified by: _____
Michael J. Cima
Sumitomo Electric Industries Professor of Engineering
Thesis Supervisor

Accepted by: _____
Christine Ortiz
Chair, Departmental Committee on Graduate Students

Emergency Delivery of Vasopressin from an Implantable MEMS Rapid Drug Delivery Device

by

Hong Linh Ho Duc

Submitted to the Department of Materials Science & Engineering
on May 6, 2009 in Partial Fulfillment of the
Requirements for the Degree of Doctor of Philosophy in
Materials Science & Engineering

ABSTRACT

An implantable rapid drug delivery device based on micro-electro-mechanical systems (MEMS) technology was designed, fabricated and validated for the *in vivo* rapid delivery of vasopressin in a rabbit model. *In vitro* characterization of device performance found the device capable of reliably and reproducibly delivering 85% of its loaded drug solution.

A comparison of intraperitoneal and subcutaneous injections of vasopressin in rabbits was performed to determine the implantation location for the device. Both routes of delivery were found to be viable implantation locations, and the less invasive subcutaneous site was chosen.

Vasopressin was released from the subcutaneously implanted device in anesthetized rabbits and found to exert a measurable effect on blood pressure. The bioavailability of vasopressin delivered from the device was found to be 6.2% after one hour.

Proof-of-concept experiments were also conducted to address long-term stability of drugs in the implanted device and wireless activation of the device. These experiments defined areas of future research for improvement of the device.

Thesis Supervisor: Michael J. Cima
Title: Sumitomo Electric Industries Professor of Engineering
Director, Lemelson-MIT Program

ACKNOWLEDGEMENTS

I would like to express the most profound gratitude to my thesis advisor, Prof. Michael Cima, for his insightful guidance during these past years. Working with him has been enlightening, and has taught me much about the way research can make a difference in medicine and healthcare.

I also have a debt of gratitude toward Dr. Noel Elman, to whom I owe much of the knowledge I have acquired about MEMS processing and fabrication.

The students in the CPRL group, past and present, have made my time at MIT enjoyable through their friendship and support, especially during the final years, and I thank them for that.

Finally, I would like to dedicate this work to the three women in my life: my mother, my wife and my daughter. They are the voice of reason, the apple of my eye and the light of my life, respectively. But more importantly, they all know how to light a fire under my bum to get me moving…

TABLE OF CONTENTS

LIST OF FIGURES

LIST OF TABLES

CHAPTER 1: INTRODUCTION

1.1. Implantable Drug Delivery Devices

Drug delivery is a broad term that refers to the method by which a drug is delivered to its site of action. The most commonly known types of drug delivery are oral (e.g. pills, syrups), topical (e.g. creams), inhalation (e.g. aerosols) and transmucosal (e.g. sublingual, ocular, rectal) delivery. They are widely used because of their non-invasiveness. Diseases or conditions which are increasingly difficult to treat require increasingly complex or potent medications, however. The available means of delivery generally become more restricted, because these complex medications become susceptible to the first-pass effect, i.e., enzymatic degradation in the digestive tract or liver, or because of difficulties in reaching target areas through the circulatory system. Vaccines and antibodies, for example, must be injected due to a large first-pass effect if ingested. Some medications must also be injected directly into their action site, because the systemic levels necessary to reach therapeutic levels in the target zone are toxic. Many cancer drugs belong in this category, such as carmustine and temozolomide. These action sites are not always accessible because of their location, or because the length and/or frequency of access necessary for therapeutic treatment greatly affect the patient's quality of life.

The brain is a difficult target zone, for example. Drug therapy targeted at the brain is difficult to achieve by systemic injection with many drugs. The blood-brain barrier hampers drug absorption from blood vessels into the brain. This barrier requires

toxic systemic drug levels to achieve therapeutic effects in the brain. Direct access is impossible without major surgery, precluding any repeated treatments. Another difficult location is the bladder. Some diseases affecting the bladder, such as interstitial cystitis, can be alleviated by direct infusion of therapeutics into the bladder, achieved by introducing a catheter through the urethra [1]. This procedure is very uncomfortable for patients and is carried out several times a week, increasing risks for urinary tract infection, and affecting quality of life.

Implanted drug delivery devices bring a solution to these problems, by delivering a drug regimen as effective as traditional therapy for extended periods of time in a particular location. They remove the necessity for frequent access and always improve quality of life for the patient compared to traditional treatments. Examples of these devices used commercially are the SynchroMed® system developed by Medtronic, Inc. for infusion of morphine directly into the cerebrospinal fluid; Gliadel®, a polymer wafer that slowly releases carmustine and is used in conjunction with resection of recurrent glioblastoma multiforme tumors in the brain; and drug-eluting stents that are widely used in angioplasty.

1.2. MEMS Technology in Drug Delivery

Micro-electro-mechanical systems (MEMS) technology is based on silicon microprocessor fabrication tools. Its ability to produce micron-sized features in substrates such as silicon, glass and polymers has made it almost ubiquitous in the production of drug delivery devices, especially for implantable devices where size is a

concern. Examples of drug delivery devices based on MEMS technology abound in the literature [2-4], but of particular interest in this work are devices fabricated in silicon.

Multi-reservoir silicon devices have been shown to release efficacious amounts of carmustine to a tumor in rats [5]. *In vivo* release of leuprolide, a polypeptide used in prostate cancer and endometriosis treatments, has also been demonstrated [6]. These multi-reservoir devices allow control of therapeutic profiles and can be either preprogrammed or activated telemetrically. Eventual integration of these devices with biosensors could result in fully automated therapeutic systems if medical personnel involvement is not necessary.

1.3. Emergency Drug Delivery

The majority of implantable drug delivery devices are used in the treatment of chronic illnesses, because they allow targeted therapeutic treatments for long periods of time while improving quality of life for patients. Much time is allowed for preparation and implantation of devices, as therapeutic profile durations are on the order of days to weeks.

Conditions with acute symptoms such as anaphylactic shock or cardiac arrest are unpredictable, although efforts have been undertaken to predict cardiac arrest [7, 8]. Therapies have to be performed within minutes of the onset of symptoms to be effective and, in some cases, to avert permanent damage or death. The only existing therapy with an implantable device is the implantable cardiac defibrillator, which can jolt a heart back to normal sinus rhythm when anomalies are detected. Drug-based therapies consist of nitroglycerin pills to be placed sublingually for patients at risk for cardiac arrest, and

Epipens® for patients susceptible to anaphylactic shock. Epipens® are spring-loaded devices that immediately deliver an intramuscular dose of epinephrine when jammed against the thigh, allowing symptom relief before reaching a hospital. These treatments require self-administration or help from another person, which is not always possible depending on the patient's condition and location. An implanted drug delivery device could ensure delivery no matter the circumstances when coupled with appropriate biosensors for a closed-loop system or when triggered by the patient for on-demand delivery. Remote health monitoring systems in the future may even allow caregivers to remotely trigger drug delivery when an emergency occurs.

An implantable rapid drug delivery device may also be useful in military conflicts. Combat conditions do not always allow emergency care to be administered to an injured soldier under heavy enemy fire. Bleeding injuries can lead to massive blood loss if untreated, leading to hemorrhagic shock, a hypotensive state of deficient organ perfusion caused by the lack of blood. Hemorrhagic shock, also known as hypovolemic shock, is the most common cause of preventable death in the Army [9]. It is treated in a civilian hospital setting by hemorrhage control, fluid replacement, and the injection of vasoconstrictors. These measures can be delayed in a combat environment, leading to death. Self-applied hemostatic dressings have been shown to help reduce bleeding on external wounds, but are not effective for internal bleeding or if too much blood has already been lost [9].

Voelckel *et al* have conducted a preclinical experiment in a pig hemorrhagic shock model where vasopressin injected intravenously was able to keep pigs alive for 30 minutes without any other intervention, whereas epinephrine and placebo could not [10].

Vasopressin, also called antidiuretic hormone, is a peptide produced in the hypothalamus and secreted by the posterior pituitary gland of most mammals [11-13]. Its primary function is to regulate the body's water retention by acting on the kidneys to reabsorb water and decrease urine output when high plasma osmolality is detected. Loss of arterial blood pressure (due for example to blood loss) triggers release of a higher concentration of vasopressin that initiates arteriolar vasoconstriction, shunting blood from the limbs and mesenteric circulation towards the heart and brain. Several case studies have illustrated the potential of exogenous vasopressin in delaying or reversing hemorrhagic shock in trauma victims [14-17]. A clinical trial has been started in January 2009 in Europe, studying the potential benefits of vasopressin therapy in traumatic hemorrhagic shock [18]. The conclusions from this study may validate the use of vasopressin in standard treatments for hemorrhagic shock. Wounded soldiers at risk for hemorrhagic shock may benefit from vasopressin only if it can be delivered in a timely manner. An implanted drug delivery device that could be remotely activated by a medic would solve the problem of access to a wounded soldier when battle conditions do not allow the medic to be physically present.

1.4. An Implantable Emergency Drug Delivery Device

The previous discussion delineates the requirements for an implantable emergency drug delivery device, beside the usual requirement of biocompatibility. These requirements are:

- ability to rapidly release drug content;
- long-term stability of drug in device; and

- wireless triggering for remote activation.

This dissertation presents the proof-of-principle for an implantable MEMS drug delivery device operating on the principle of bubble nucleation to rapidly release its drug loading. Vasopressin was chosen as a model drug for delivery not only because of its potential benefits in hemorrhagic shock, but also because of its expanding use in cardiac arrest [19, 20]. The device design, fabrication and *in vitro* characterization are discussed in Chapter 2 and have been published in an article co-authored with Dr. Noel Elman [21]. The selection of a candidate location for implantation through pharmacokinetic measurements is described in Chapter 3, and *in vivo* testing of the device in the selected location is reported in Chapter 4. Part of the work presented in both these chapters has been submitted for publication. This work has focused primarily on the rapid delivery component of the device, but Chapter 5 offers some early experiments geared towards long-term stability of the drug and wireless activation.

1.5. References

1. Theoharides, T.C., *Treatment approaches for painful bladder syndrome/interstitial cystitis.* Drugs, 2007. **67**(2): p. 215-235.
2. Grayson, A.C.R., et al., *A BioMEMS review: MEMS technology for physiologically integrated devices.* Proceedings of the Ieee, 2004. **92**(1): p. 6-21.
3. Bashir, R., *BioMEMS: state-of-the-art in detection, opportunities and prospects.* Advanced Drug Delivery Reviews, 2004. **56**(11): p. 1565-1586.
4. Tsai, N.-C. and C.-Y. Sue, *Review of MEMS-based drug delivery and dosing systems.* Sensors and Actuators A: Physical, 2007. **134**(2): p. 555-564.
5. Li, Y.W., et al., *In vivo delivery of BCNU from a MEMS device to a tumor model.* Journal of Controlled Release, 2005. **106**(1-2): p. 138-145.
6. Prescott, J.H., et al., *Chronic, programmed polypeptide delivery from an implanted, multireservoir microchip device.* Nature Biotechnology, 2006. **24**(4): p. 437-438.
7. Pai, J.K., et al., *Inflammatory markers and the risk of coronary heart disease in men and women.* New England Journal of Medicine, 2004. **351**(25): p. 2599-2610.
8. Wang, T.J., et al., *Multiple biomarkers for the prediction of first major cardiovascular events and death.* New England Journal of Medicine, 2006. **355**(25): p. 2631-2639.
9. Alam, H., E. Koustova, and P. Rhee, *Combat casualty care research: from bench to the battlefield.* World J Surg, 2005. **29**: p. S7-S11.
10. Voelckel, W.G., et al., *Arginine vasopressin, but not epinephrine, improves survival in uncontrolled hemorrhagic shock after liver trauma in pigs.* Critical Care Medicine, 2003. **31**(4): p. 1160-1165.
11. Henderson, K.K. and K.L. Byron, *Vasopressin-induced vasoconstriction: two concentration-dependent signaling pathways.* J Appl Physiol, 2007. **102**(4): p. 1402-1409.
12. den Ouden, D.T. and A.E. Meinders, *Vasopressin: physiology and clinical use in patients with vasodilatory shock: a review.* Netherlands Journal of Medicine, 2005. **63**(1): p. 4-13.
13. Treschan, T.A. and J. Peters, *The vasopressin system - Physiology and clinical strategies.* Anesthesiology, 2006. **105**(3): p. 599-612.
14. Haas, T., et al., *Successful resuscitation of a traumatic cardiac arrest victim in hemorrhagic shock with vasopressin: A case report and brief review of the literature.* Journal of Trauma-Injury Infection and Critical Care, 2004. **57**(1): p. 177-179.
15. Krismer, A.C., et al., *Employing vasopressin as an adjunct vasopressor in uncontrolled traumatic hemorrhagic shock - Three cases and a brief analysis of the literature.* Anaesthesist, 2005. **54**(3): p. 220-224.
16. Sharma, R.M. and R. Setlur, *Vasopressin in hemorrhagic shock.* Anesthesia and Analgesia, 2005. **101**(3): p. 833-834.
17. Tsuneyoshi, I., et al., *Low-dose vasopressin infusion in patients with severe vasodilatory hypotension after prolonged hemorrhage during general anesthesia.* Journal of Anesthesia, 2005. **19**(2): p. 170-173.

18. Wenzel, V., *Vasopressin in Traumatic Hemorrhagic Shock Study*. 2009, ClinialTrials.gov.
19. *2005 American Heart Association Guidelines for Cardiopulmonary Resuscitation and Emergency Cardiovascular Care - Part 7.2: Management of Cardiac Arrest.* Circulation, 2005. **112**(24_suppl): p. IV-58-66.
20. Wenzel, V., et al., *A Comparison of Vasopressin and Epinephrine for Out-of-Hospital Cardiopulmonary Resuscitation.* N Engl J Med, 2004. **350**(2): p. 105-113.
21. Elman, N.M., H.L. Ho Duc, and M.J. Cima, *An Implantable MEMS Drug Delivery Device for Rapid Delivery in Ambulatory Emergency Care.* Biomedical Microdevices, 2009. **In press**.

CHAPTER 2: DEVICE FABRICATION AND CHARACTERIZATION

2.1 Introduction

Implantable drug delivery devices have demonstrated their great potential in a vast number of applications for which the controlled and accurate delivery of critically prescribed drug doses is required without direct medical intervention. A variety of implantable devices based on Micro-Electro-Mechanical-Systems (MEMS) technology has already been demonstrated for chronic illnesses. These devices include micro-pumps [1] and multi-reservoir silicon chips [2, 3], for example. Actively controlled devices provide advantages over passive release devices, which rely on the degradation chemistry of the device materials or on osmotic processes to release their load [4-6], as the drug delivery process can be controlled actively after implantation and even engaged telemetrically.

MEMS technology has allowed the successful miniaturization of micro-pumps for drug delivery, enabling active delivery of fluids from single or multiple reservoirs. Low delivery rates, low reliability due to the dependence on mechanical moving parts in fluids, and high power consumption are among the prime limitations of an implantable drug delivery device that relies on micro-pumps. Drug delivery devices characterized by multiple-reservoir architectures and based on electrical actuation mechanisms provide a more reliable platform. These devices typically rely on electro-thermal actuation to

rupture a reservoir sealing membrane as a result of an applied electrical potential, allowing the drugs inside of reservoirs to freely diffuse into the region of interest [7].

A number of implantable drug delivery devices have been investigated for use in chronic and non-chronic diseases in ambulatory settings without medical intervention, such as cancer, diabetes, and osteoporosis [8]. These implantable devices provide a significant improvement in the bioavailability of drugs, but their use is mainly limited to treatment of chronic illnesses as they rely on diffusion and small delivery volumes, with complete release achieved in a few hours. Current implantable drug delivery devices based on MEMS technology are therefore not adequate as a solution for immediate treatment of illnesses in trauma care. None of the currently available technologies for implantable drug delivery devices fulfill the requirements for rapid *in vivo* treatment of pathologies in emergency situations. The challenge lies in the implementation of an active drug delivery device capable of storing large volumes, preferably without any moving parts to increase performance reliability, and mainly characterized by high delivery rates to achieve treatment in a few minutes as opposed to a few hours. The development of implantable devices for emergency treatments that require rapid and reliable drug delivery is thus the main motivation of this work.

This chapter presents the first rapid drug delivery platform suitable for implementation as a smart micro-implant for high-risk patients. This novel device can be useful for a number of delivery modalities, including subcutaneous, intraperitoneal, intramuscular, and transdermal delivery. Potential pathologies that the device can address with patients at high risk include cardiac arrest, angina, anaphylactic shock and epilepsy. The device's goal is to provide a drug bolus in minutes or less upon triggering.

The work presented in this chapter has been published in Biomedical Microdevices [9] and is reproduced here with kind permission from Springer Science + Business Media, LLC.

2.2. Device Architecture

The modular device architecture allows separation of device opening and drug expulsion mechanisms, as well as customization of the drug load volume. The architecture is shown schematically in Figure 2.1 and is comprised of three layers: a Pyrex single reservoir layer, where the drug solution is stored; a membrane layer that hermetically seals the drug reservoir, and from where the drug is ejected; and an actuation layer carrying the drug expulsion mechanism.

The Pyrex macroreservoir is fabricated by drilling circular holes in a Pyrex 7740 wafer. Capacity is defined by the diameter of the drilled hole (3.6 mm) and thickness of the wafer (2.25 mm), and is currently 22.9 μL. The modular design of the chip allows the capacity to be changed simply by changing the dimensions of the drilled hole, either by using a different thickness wafer or by changing the diameter of the hole.

The membrane layer consists of free-standing silicon nitride membranes over square silicon through-wafer vias with dimensions 400 x 400 μm. Silicon nitride is commonly used as a diffusion-stop layer in silicon technologies and prevents diffusion in or out of the reservoir, keeping the drug solution sealed until needed. A gold line is patterned on top of the membrane to detect membrane rupture. The gold circuit opens when the membrane, and consequently the gold line, is ruptured. This allows membrane opening detection by monitoring the resistance across the line for an open-circuit.

The actuation layer contains patterned titanium resistors. A current passed through the resistors produces heat by virtue of the Joule effect, generating thermal vapor bubbles in the solution. These bubbles increase pressure inside the macroreservoir, until a silicon nitride membrane on the top chip ruptures. The contents of the macroreservoir are then expelled out of the device due to the volume expansion that the vapor bubbles create, allowing the delivery of 20 μl of solution in 45 seconds of current application.

All materials of construction of this device (silicon, silicon nitride, silicon dioxide, gold and titanium) have been shown to be biocompatible [10, 11]. The device operational design and principles are introduced, followed by experimental validation to address its performance characteristics.

2.3. Device Design

Bubble nucleation by heating a liquid is a well-known phenomenon, and can be initiated by electrically heating a resistive element to generate localized boiling. The sudden increase in pressure bursts a sealing membrane, thereby releasing the drugs at a high rate. The design of the actuation layer is therefore critical for the performance of the device. The actuation layer consists of three resistive elements in parallel. The resistor area was designed to be compact in order to localize the heat transfer. The power density (amount of power per surface unit area of the resistor) was designed to reach approximately 25 W/mm^2 in order to exceed the nucleate boiling threshold and enter the film boiling regime for water [12]. Film boiling is desired in order to insulate the bulk of the drug solution from the resistor surface, and prevent drug degradation due to overheating. Titanium was chosen as material for the resistive element because it is

biocompatible and characterized by a relatively high resistivity for metals. This allows it to be patterned with the desired area while avoiding overly thin layers (< 200 Å) that might be needed with more conductive metals such as gold in order to achieve the appropriate resistances. Three U-shaped resistors of 30 Ohms capable of delivering the required power density were designed to connect in parallel to achieve a 10-Ohm electrical resistance. The thickness was optimized to achieve the desired resistor values in order to compensate for impurities in the Ti due to the deposition process. This step involved deposition of several thicknesses of Ti and subsequent measurements of sheet resistance using a four-point probe (Keithley SCS-4200, Keithley Instruments Inc., USA). The resultant thickness was 250 nm, providing a sheet resistance of 2.7 Ω/□.

The membrane layer consists of a free-standing silicon nitride membrane that acts as a hermetic seal preventing both the drug inside of the reservoir to diffuse out, and any foreign substance to penetrate inside of the reservoir. Silicon nitride was chosen as the membrane material due to its high density and use as a diffusion-stop layer. Its mechanical properties allow limited elastic deformation while maintaining a hermetic seal. The membrane shatters into small fragments when the silicon nitride membrane is subjected to a critical pressure. The membrane dimensions were optimized to withstand external pressure and stresses involved in the handling and implantation of the device, but also to allow the membrane to burst when activation of the device increases pressure inside the device. A design based on a square membrane was chosen for its simplicity in implementation. A finite element analysis (FEA) tool (Cosmos, SolidWorks, Inc., USA) was used to simulate the failure points based on applied pressures for different membrane lateral dimensions, keeping the thickness to a constant 200 nm. The stresses were

simulated using the Von Mises method and the theoretical maximum tensile stress of amorphous silicon nitride (200 MPa), and meshed with $3x10^5$ elements. The results of the simulation revealed that a 400-μm square membrane can withstand normal pressures of up to 5kPa, while maintaining an acceptable factor of safety. Calculations based on standard analytical solutions [13] also reveal that the chosen membrane dimensions are structurally robust for this application.

2.4. Fabrication Process

The device fabrication is comprised of three separate processes: the membrane layer, the reservoir layer, and the actuation layer. These processes are independent due to the modular architecture of the device, as was shown in Figure 2.1. The process for fabrication of these separate layers referred hereinafter is described in Figures 2.2 and 2.3.

2.4.1. Membrane Layer

The membrane layer comprised of an array of standing SiN membranes is combined with patterned gold fuses, which are designed to act as sensors. A fuse is broken when a membrane is burst, resulting in an open circuit that can be detected by measuring the fuse resistance. The membrane layer was fabricated using micro-machining technology. A 500 nm thermal silicon dioxide (SiO_2) layer is grown on a 100 mm, double polished, 300 μm thick, single-crystal-silicon (SCS) wafer, followed by deposition of a 200 nm layer of SiN by low-pressure vapor chemical deposition (LPCVD). A 30 nm titanium adhesion layer and a 300 nm gold layer are then sputter-deposited. The first photolithographic step then defines the electrical fuses on top of the

membranes. Gold and titanium are wet etched to form the fuses, shown in Figure 2.2A. The patterned wafer is then coated with a layer of photoresist for protection. The backside of the wafer is photolithographically patterned to define the silicon nitride membranes. CF_4-based reactive ion etching (RIE) first transfers the pattern to the backside SiN and SiO_2 layers, then deep RIE based on the Bosch^{TM} process is performed to anisotropically etch through the wafer up to the front-side buried SiO_2 layer, shown in Figure 2.2B. This layer acts as a stop mask, and allows compensation for approximately 10 percent etch non-uniformity commonly seen in the deep RIE processes [14]. The wafer is finally dipped in 49% HF for 2 minutes to remove the remaining oxide and release the silicon nitride membranes. The wafers are then diced into 5 mm x 5 mm chips.

2.4.2. Actuation Layer

The actuation layer was also fabricated using micro-machining technology on 100 mm SCS substrates. The process sequence is shown in Figure 2.3. The first step is to grow a 500 nm thermal SiO_2 layer, which serves to electrically isolate the substrate. A 250 nm Ti layer followed by a 300 nm Au layer are sputtered next, shown in Figure 2.3A. The first photolithographic process is implemented to pattern Au electrical contacts, and is followed by Au and Ti wet etches to define the electrode layer shown in Figure 2.3B. The next steps are designed to encapsulate the resistors for protection against subsequent etch steps, and provide a robust adhesion layer for oxide deposition. Sputtering of 300 nm of Au and 20 nm of Ti is followed by the second photolithographic step. Ti and Au layers are then wet-etched sequentially to define a capsule around the resistors, Figure 2.3C. The next step is to conformally deposit 2 μm of SiO_2 to isolate the electrodes

layers and prevent electrolysis between electrodes once the device is fully packaged and operating, Figure 2.3D. The third photolithographic step is implemented to define vias for bonding pads in the electrodes, and open areas around the resistors. A CF_4-based RIE is used to etch SiO_2 and the Ti adhesion layer to expose the bonding pads and the resistors. The last photolithographic step masks the bonding pads. This step is followed by an Au etch, finally exposing the Ti resistors. The wafer is diced into 5 mm x 9 mm chips.

2.4.3. Reservoir Layer

The reservoir layer was defined using 100 mm, double-polished, 2.25 mm thick Pyrex 7740 wafers. These wafers were drilled using a 1.7 mm radius diamond bit to achieve a reservoir volume of 20 μL, and diced in 6 mm x 8 mm chips.

2.4.4. Device Assembly and Loading

All three layers were bonded together using a biocompatible UV-cured epoxy (1-20542 cationic epoxy, Dymax Corporation, Torrington, CT). The layers can also be anodically bonded for permanent hermeticity. The chip was loaded by breaking one of the nitride membranes and dispensing solutions with known drug concentration through the opening using a 100 μL syringe with a 32 Gauge needle (Hamilton Company, Reno, NV), mounted in an injection system consisting of a UMP-1 Ultra Micro Pump with Micro-1 controller and a Kite-R micromanipulator with a TB-1 tilting base (all from World Precision Instruments, Sarasota, FL). This system allows precise control of the amount of solution injected into the device, and by extension, the amount of loaded drug.

The open membrane was subsequently sealed with UV-cured epoxy. Electrical wires and connectors were connected to the chip and wire-bonding was performed to connect the electrical wires to the chips. The final packaged device is shown in Figure 2.4.

2.5. Experimental Methods

Three sets of experiments were conducted to validate the device. The first experiment consisted of electrical characterization of the device *in vitro* by releasing a dye. Such a test was necessary to empirically determine the power consumption of the device and qualitatively determine the release rates. The second experiment consisted of quantitatively determining the release rates using radio-labeled vasopressin. The third experiment consisted of quantitatively determining the effects of the actuation mechanism (localized bubble nucleation) on drug degradation using high-pressure liquid chromatography (HPLC).

2.5.1. Electrical Characterization

The devices were first tested *in vitro* by releasing methylene blue to determine the I-V curve characteristics while optically recording the release event. The devices were placed inside of a 10 mL beaker filled with deionized (DI) water. An increasing DC voltage was applied to the heating elements using a voltage source, and the current was measured. The device was optically inspected and recorded using a video camera connected to a stereoscope to register the conditions under which the dye was delivered.

2.5.2. Quantification by Radioactive Release

The amount of volume released by the device was determined using a solution of arginine vasopressin (Sigma-Aldrich, Inc., St. Louis, MO) and ^{3}H-radiolabeled arginine vasopressin (American Radiolabeled Chemicals, Inc., St. Louis, MO). Four devices were filled with 20 μL of radiolabeled solution following the procedure described above. An additional three controls were injected directly into water to be measured and determine the loading in all devices. The test devices were activated for 45 seconds with an applied voltage of 9 V in 2 mL of DI water. The media was sampled immediately before and after each device activation. Media aliquots were measured in a liquid scintillation counter (Packard Tri-Carb 2200CA, Perkin-Elmer Life Sciences, Waltham, MA) to determine the fraction of original loading that was released.

2.5.3. Quantification by HPLC

The effect of device actuation on the degradation of vasopressin was determined in three devices. The devices were filled with 20 μL of a 25 mg/mL solution of arginine vasopressin and sealed. Another 20 μL of solution was also directly injected into 5 mL of DI water as control, resulting in a concentration of 0.1 mg/mL. Devices were activated as in the previous section in 5 mL of DI water and media samples were collected immediately after activation. Samples were analyzed by reverse-phase HPLC (RP-HPLC), using an Agilent 1200 Series with quaternary pump and diode array detector (Agilent, Inc., Santa Clara, CA). A gradient method was used in a Brownlee Spheri-ODS column (25 cm x 4.6 mm, 5 μm, 100 Å, Alltech Associates, Deerfield, IL), with methanol and 0.1% trifluoroacetic acid (TFA) in water both obtained from Sigma-Aldrich, Inc. (St.

Louis, MO). The gradient used was 2 % TFA/min, starting at 0%. The flow rate was 1 mL/min and the detection wavelength 220 nm. The Chemstation software (Agilent, Inc., Santa Clara, CA) was used to measure the area under the observed retention peaks and calculate the area fraction of the vasopressin peak, yielding the fraction of intact vasopressin.

2.6. Results

2.6.1. Electrical Characterization

Figure 2.5 shows the I-V curve of the heating elements. The red circle indicates that the device is intended for 9 V operation. Bubbles were observed for an applied DC voltage of 9 V and the measured current was approximately 650 mA. Figure 2.6 shows the methylene blue jetted into DI water during actuation. The electrical fuses on top of the membranes were also monitored during each activation and were observed to become open-circuited as the membranes burst, proving that it is possible to interrogate the device by means of impedance measurement to check whether the sealing membrane is opened by the device actuation.

2.6.2. Radioactive Release Quantification

Figure 2.7 shows the measured loading fraction released after each activation. The results indicate that 92.9 ± 0.7 % (n = 4) of the original loading was released by the devices.

2.6.3. HPLC Quantification

Vasopressin was found to have a retention time of 16.8 minutes. The area fraction of the vasopressin peak for the devices was compared to that of the control, and it was found that 9.0 ± 0.7 % (n = 3) of the vasopressin released by the devices was degraded with respect to the original state of vasopressin injected into the devices, as shown in Figure 2.8.

2.7. Discussion

The device designed and fabricated in this work is an implantable device based on MEMS technology that provides a platform for applications requiring rapid drug delivery. The best candidates for this device are conditions of an urgent nature that would require a depot, but not necessarily intravenous access. The actuation mechanism of the device is similar to inkjet printing, as it relies on film micro-boiling, but the volumes of liquid to be displaced are six orders of magnitude greater. The resistors involved in the bubble nucleation process were designed to guarantee that the nucleation occurs in the film boiling regime. The power density achieved is approximately 25 W/mm^2 allowing an effective increase in the reservoir pressure, while guarantying that the bubble nucleation is in the film boiling regime. Electrical characterization showed that activation requires relatively high power for an implantable device, approximately 6 W for 45 seconds, but this device can be connected to commercially available ultra-high density capacitors, which can provide 240 J from a very small size component to power it. Future generations of this device should try to reduce power consumption, notably by improving insulation of the device to reduce heat losses to the environment.

The degradation study by HPLC demonstrated that the heating involved in the actuation of the device does not significantly affect vasopressin *in vitro*, as 91 ± 0.7 % of the drug was still effective after release. Quantification of device loading fraction released by radiolabeled vasopressin determined that 92.9 ± 0.7 % of the loaded solution was released in 45 seconds. It can therefore be inferred by simple multiplication of these two measurements that 84.5 ± 0.9 % of the drug originally loaded into the device is released in its active form. An overhead volume can thus be included when loading the device in order to deliver a consistent target dose.

A potential issue related to the use of this device is the presence of silicon nitride fragments after activation. One may worry that these fragments may damage surrounding tissue at the moment of membrane bursting or thereafter. The mass of a 400 x 400 x 0.2 μm piece of silicon nitride with a density of 3.4 g/cm^3 is 0.11 ng. It is unlikely that such a mass, upon bursting, would be able to significantly damage tissue around the device. The fragments released after activation of the device are not expected to travel from the implantation site, and would eventually be surrounded by a fibrous capsule and isolated from the body. Their presence is therefore not anticipated to be a problem. *In vivo* testing of the device may bring answers to these questions, although the small size of the fragments may render this task difficult.

Another solution to the problem is to use gold membranes instead of silicon nitride. A gold membrane can be melted by passing a current pulse through it, as has been demonstrated in the past [7]. The limitation of this solution is the upper limit on size of gold membrane that ensured its mechanical integrity. A dimension of 400 x 400

μm is not achievable in this author's experience, and smaller openings may affect the performance of the device. An optimization study may answer the question, however.

2.8. Conclusions

This device represents the first implantable drug delivery device specifically designed to rapidly provide medication. It is a technology platform that can be leveraged for a large number of medical applications. It was shown to provide consistent drug delivery without any major degradation in the case of vasopressin. It is an ideal candidate for pathologies that require immediate and ambulatory treatment of high-risk individuals, and allows for rapid and effective treatment. Application of this technology platform can significantly improve survival rates in ambulatory settings.

2.9. Figures

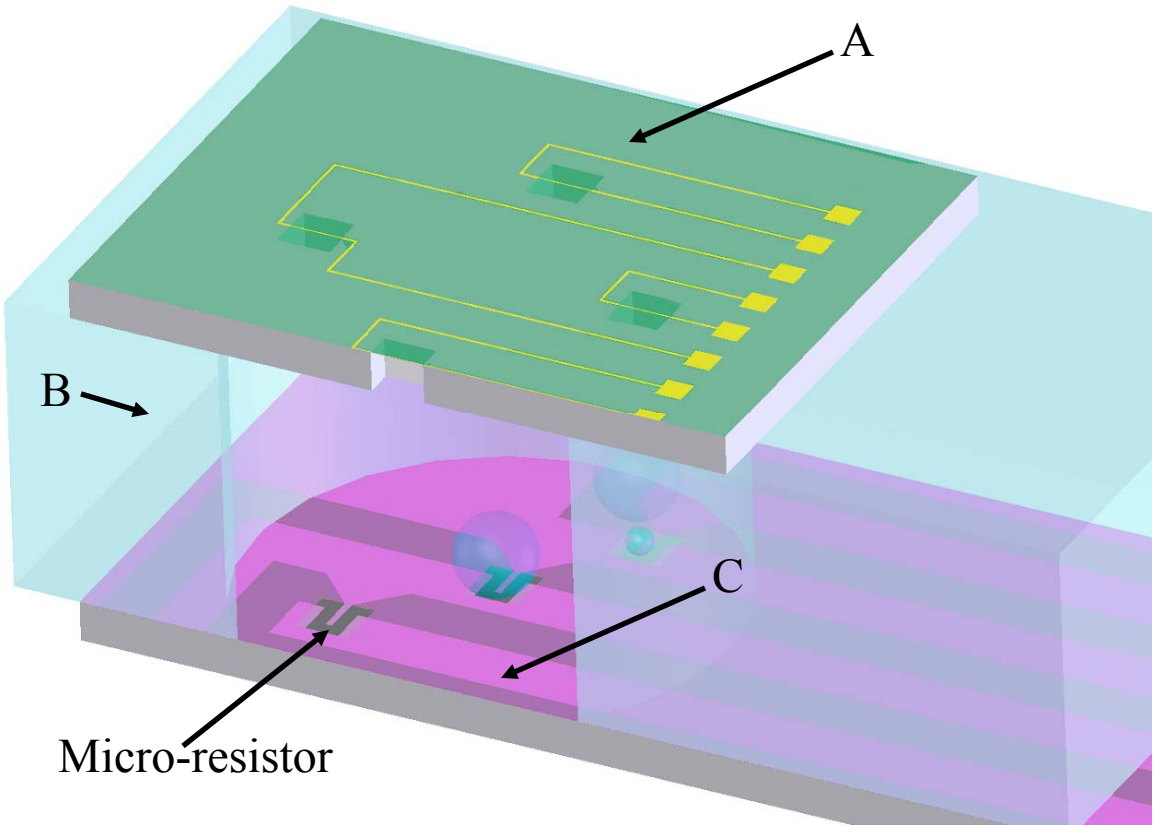

Figure 2.1: Cross section of the device showing the three layers: membrane layer (A), reservoir layer (B) and actuation layer (C).

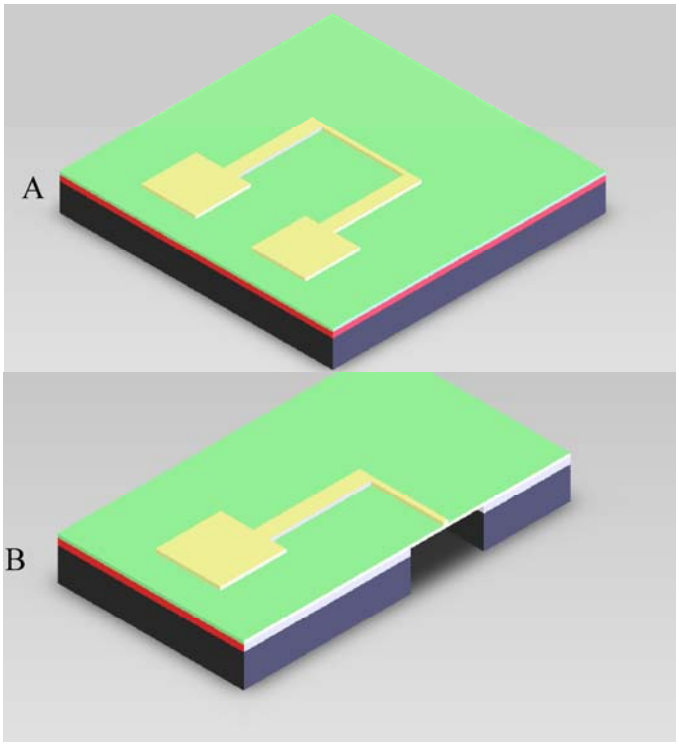

Figure 2.2: Fabrication sequence for the membrane layer. (A) Electrodes on Au, deposited on Si_3N_4 (green) and SiO_2 (red), followed by (B) through-wafer via etching by DRIE.

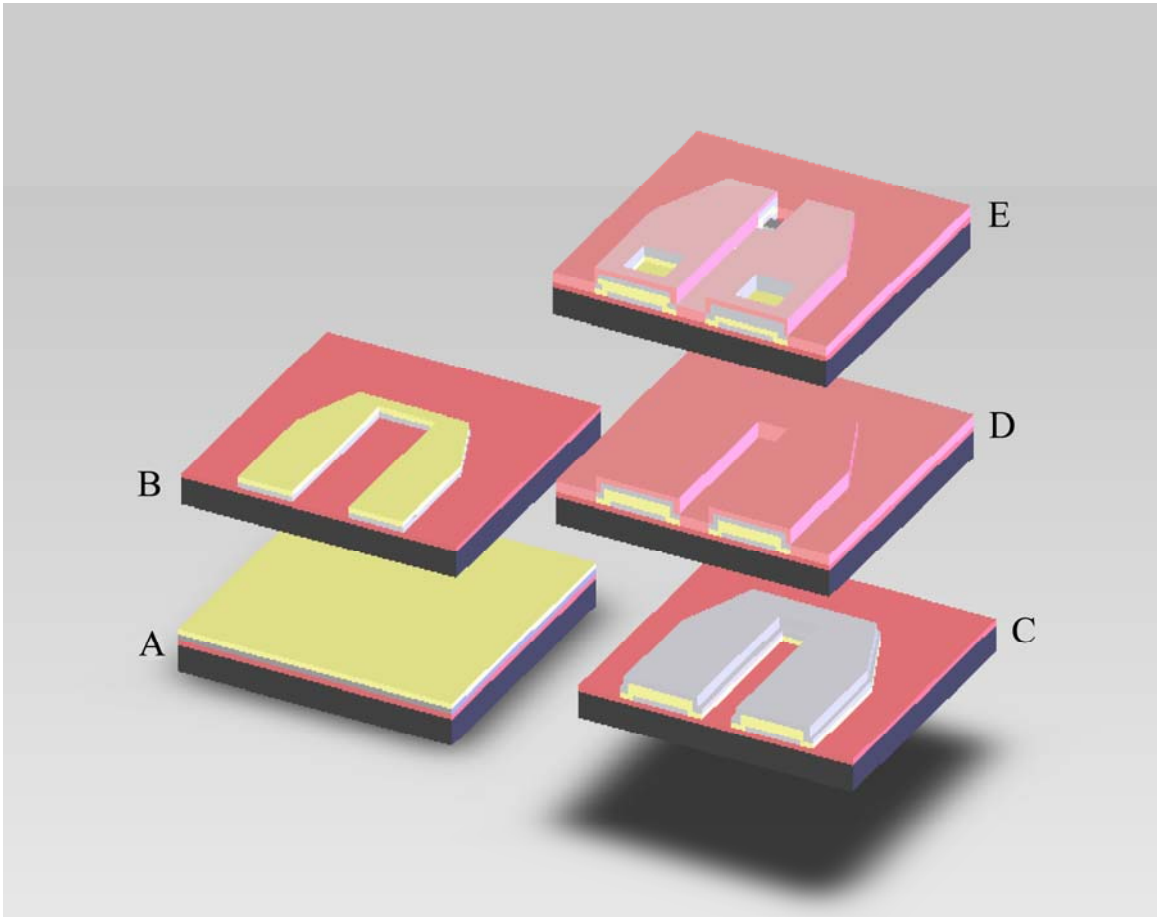

Figure 2.3: Fabrication process of actuation layer. (A) SiO_2, Ti, Au deposition on SCS substrate. (B) Definition of electrodes and resistor. (C) Ti, Au encapsulation. (D) SiO_2 deposition. (E) Electrodes vias and exposure to Ti resistor.

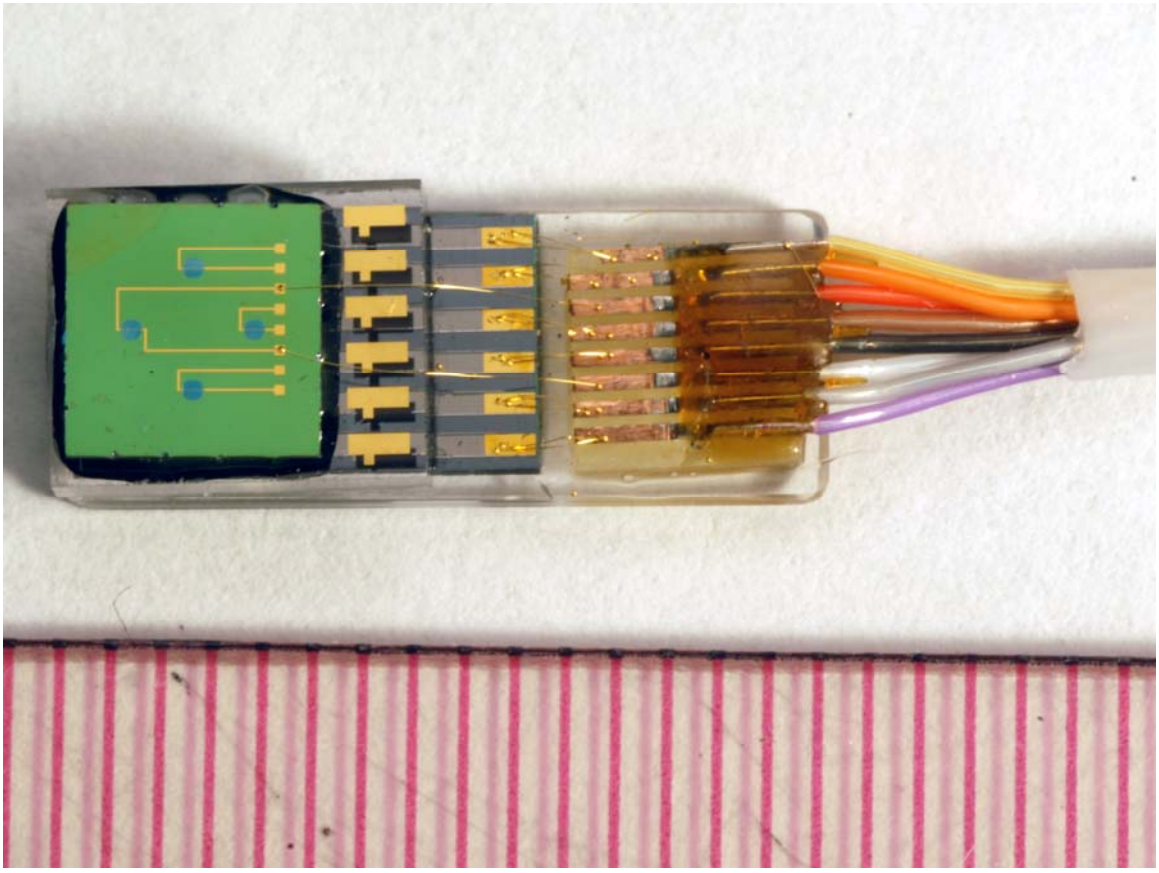

Figure 2.4: Final packaged device showing the top chip with four silicon nitride membranes. The device is wirebonded to detect opening of the far left membrane and to apply current to the microresistors. Ruler graduations are in millimeters.

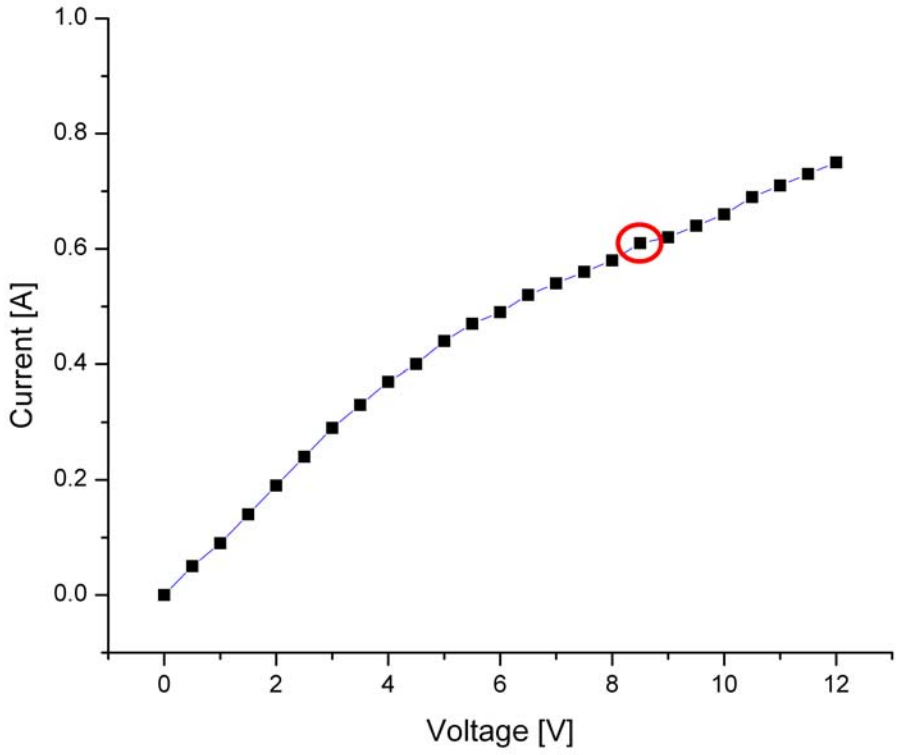

Figure 2.5: I-V curve of the device. The device was designed to be active at 9 V, indicated in red.

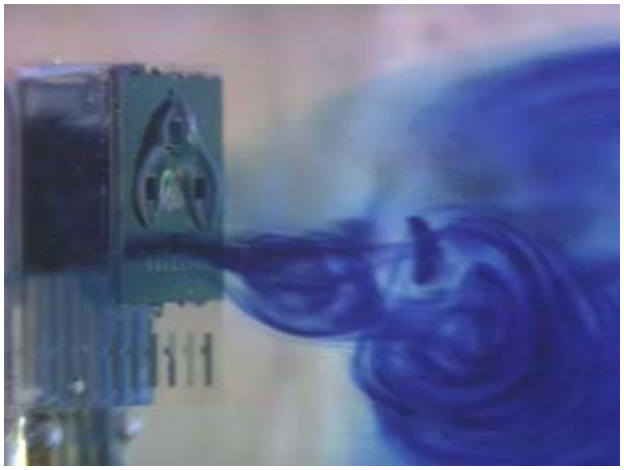

Figure 2.6: Side view of device showing release of methylene blue into a solution upon activation.

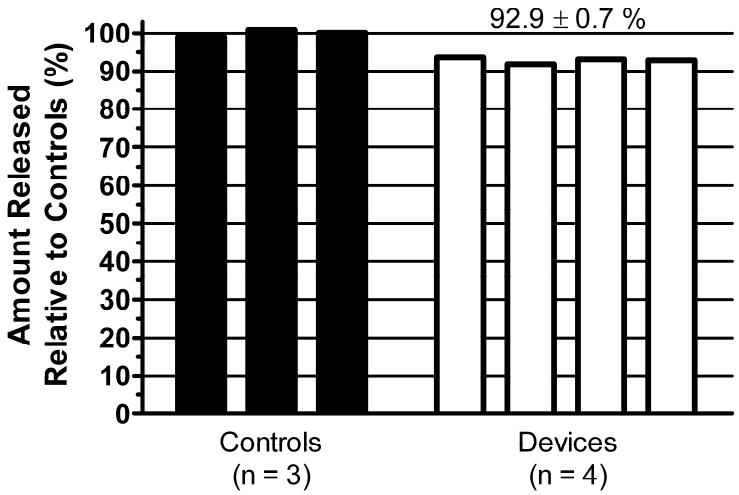

Figure 2.7: Quantification of vasopressin release by radiolabeled species.

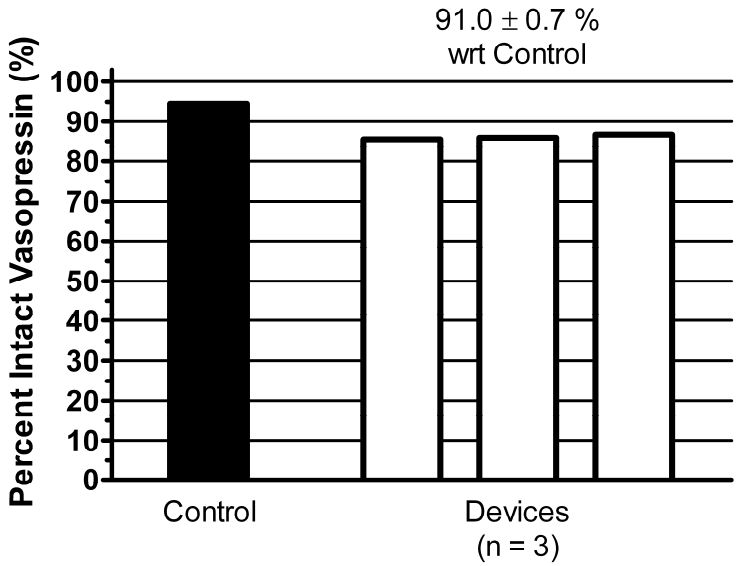

Figure 2.8: HPLC analysis of released vasopressin from the device.

2.10. References

1. Nguyen, N.T., X.Y. Huang, and T.K. Chuan, *MEMS-micropumps: A review.* Journal of Fluids Engineering-Transactions of the Asme, 2002. **124**(2): p. 384-392.
2. Li, Y.W., et al., *In vivo delivery of BCNU from a MEMS device to a tumor model.* Journal of Controlled Release, 2005. **106**(1-2): p. 138-145.
3. Prescott, J.H., et al., *Chronic, programmed polypeptide delivery from an implanted, multireservoir microchip device.* Nature Biotechnology, 2006. **24**(4): p. 437-438.
4. Grayson, A.C.R., et al., *Multi-pulse drug delivery from a resorbable polymeric microchip device.* Nature Materials, 2003. **2**(11): p. 767-772.
5. LaVan, D.A., T. McGuire, and R. Langer, *Small-scale systems for in vivo drug delivery.* Nature Biotechnology, 2003. **21**(10): p. 1184-1191.
6. Lo, R., et al. *A Passive Refillable Intraocular MEMS Drug Delivery Device*. in *Microtechnologies in Medicine and Biology, 2006 International Conference on*. 2006.
7. Maloney, J.M., et al., *Electrothermally activated microchips for implantable drug delivery and biosensing.* Journal of Controlled Release, 2005. **109**(1-3): p. 244-255.
8. Staples, M., et al., *Application of micro- and nano-electromechanical devices to drug delivery.* Pharmaceutical Research, 2006. **23**(5): p. 847-863.
9. Elman, N.M., H.L. Ho Duc, and M.J. Cima, *An Implantable MEMS Drug Delivery Device for Rapid Delivery in Ambulatory Emergency Care.* Biomedical Microdevices, 2009. **In press**.
10. Kotzar, G., et al., *Evaluation of MEMS materials of construction for implantable medical devices.* Biomaterials, 2002. **23**(13): p. 2737-2750.
11. Voskerician, G., et al., *Biocompatibility and biofouling of MEMS drug delivery devices.* Biomaterials, 2003. **24**(11): p. 1959-1967.
12. Stralen, S.v. and R. Cole, *Boiling phenomena : physicochemical and engineering fundamentals and applications*. Series in thermal and fluids engineering. Vol. 1. 1979, Washington: Hemisphere Pub. Corp.
13. MaierSchneider, D., J. Maibach, and E. Obermeier, *A new analytical solution for the load-deflection of square membranes.* Journal of Microelectromechanical Systems, 1995. **4**(4): p. 238-241.
14. Elman, N.M., et al., *Multiple aspect-ratio structural integration in single crystal silicon (MASIS) for fabrication of transmissive MOEMS modulators.* Microsystem Technologies-Micro-and Nanosystems-Information Storage and Processing Systems, 2008. **14**(2): p. 287-293.

CHAPTER 3: *IN VIVO* PHARMACOKINETICS OF VASOPRESSIN

3.1. Introduction

The emergency delivery of vasopressin has one important requirement. It must achieve systemic therapeutic levels as quickly as possible without direct intravenous delivery because a drug delivery device cannot currently deliver directly to the bloodstream. An implanted device should therefore be placed in a location where the released drug is able to enter the circulatory system quickly. Two candidate locations have been chosen for this study, the mesentery and a subcutaneous location.

The mesentery is a highly vascularized region of the peritoneum, the lining of the abdominal cavity that envelops and protects the soft organs within it. The mesentery attaches the gastrointestinal organs to the abdominal wall and supplies them with blood. A device placed in this region could release vasopressin and allow it to enter the bloodstream quickly. Access to this location is invasive, however, as a surgery would most probably be needed to implant the device. Future generations of the device may be able to shrink it to dimensions allowing it to be inserted with a catheter or other means without requiring major surgery. Interest in this location may therefore still be warranted.

The most non-invasive location to implant a device would be subcutaneous, in an arm or a leg, as the device could easily be implanted and retrieved later without major surgery. A subcutaneous location is more peripheral than the peritoneum, however, and may not allow sufficient access to the circulatory system. Desmopressin, a synthetic

vasopressin analogue with more specific anti-diuretic activity than vasopressin, has been used as a subcutaneous injection to control the frequent urination associated with diabetes insipidus (water diabetes) and chronic bedwetting [1]. It is also used subcutaneously for at-home self-treatment of some patients with bleeding disorders such as von Willebrand disease or mild hemophilia A [2, 3]. There is thus reason to believe that subcutaneous delivery of vasopressin may be able to achieve a systemic effect.

The work presented hereinafter aims to investigate the pharmacokinetics of vasopressin injected into two candidate locations for implantation of an emergency drug delivery device. Vasopressin was injected intraperitoneally into the mesentery and subcutaneously, and its effect on blood pressure in rabbits was evaluated. Plasma levels of vasopressin were measured using radiolabeled vasopressin in order to corroborate with blood pressure and heart rate measurements. They were also used to estimate bioavailability of these injection routes.

3.2. Materials and Methods

3.2.1. Animals

This study was approved by MIT's Committee on Animal Care and the Animal Care and Use Review Office from the Department of Defense Medical Research and Material Command. Twenty-two male New Zealand White rabbits with weights between 2.5 kg and 3.5 kg were obtained (Covance Research Products, PA). The animals were housed in compliance with MIT's Committee on Animal Care husbandry guidelines, with unrestricted access to water and food.

3.2.2. Vasopressin

Arginine vasopressin acetate powder (Sigma-Aldrich, Saint-Louis, MO) was reconstituted with sterile water to appropriate concentration for injection. ^{3}H-radiolabeled vasopressin (American Radiolabeled Chemicals, St. Louis, MO) was added to injection solutions for determination of plasma levels of vasopressin.

3.2.3. Intraperitoneal Catheters

Rabbits chosen to receive intraperitoneal injections were implanted with a sterile vascular access port (VAP) (Access Technologies, Skokie, IL), consisting of a silicone catheter and a polysulfone injection port with a silicone septum. A laparotomy was performed to fix one end of the catheter to the connective tissue 1 cm from the root of the mesenteric arterial tree of the small intestine. The other end was tunneled subcutaneously along the flank to the dorsum. The injection port was fixed subcutaneously with sutures in a location caudal to the left shoulder blade through a dorsal skin incision and connected with the catheter. Figure 3.1 illustrates the final configuration of the VAP. This setup allows solutions to be injected into the peritoneum reproducibly with a syringe. The clearance volume of the port and catheter is 400 μL. All incisions were closed and rabbits were allowed to recover from the implantation surgery for a minimum of 7 days with appropriate analgesia and prophylaxis, before any injection experiments were performed.

3.2.4. Vasopressin Injections

Rabbits were anesthetized with an initial dose of midazolam (2 mg/kg, intravenous) and were maintained under anesthesia by mask with 1-3% isoflurane in balance oxygen. One ear was catheterized for intravenous access, while the central auricular arteries in both ears were catheterized for mean arterial pressure (MAP) monitoring and blood sampling, respectively. The rabbits were monitored for up to 1 hour after the start of data acquisition to let MAP stabilize to baseline before injecting vasopressin.

Rabbits received 1 μg/kg vasopressin intravenously (IV001 group, n = 11), 10 μg/kg intraperitoneally (IP010 group, n = 16), or 100 μg/kg subcutaneously (SQ100 group, n = 5). Sterile water was also injected intraperitoneally (IP000, n = 8) and subcutaneously (SQ000, n = 4) as placebo. Rabbits were monitored for 1 hour following injection or activation then euthanized by sodium pentobarbital injection. Rabbits allowed to wake up were left to recover for 7 to 14 days then received another injection. The total number of injections a rabbit received varied between 1 and 3.

MAP was monitored and recorded continuously by direct blood pressure measurement from an arterial catheter in the central auricular artery, using a Blood Pressure Analyzer^{TM} 400 with DMSI software (Micro-Med, Louisville, KY). Values were measured every 0.5 seconds and averaged over 10 seconds to yield a single data point.

ΔMAP was defined as the difference between MAP and baseline MAP, which is the average MAP measured over 5 minutes before injection. Plots of each injection were subsequently analyzed (Excel 2003, Microsoft, Inc., USA) to extract the maximum

ΔMAP (ΔMAP_{max}), the time needed to reach that maximum (t_{max}), and the time at which ΔMAP returned under baseline level for at least 1 minute thereafter (t_{dur}). Intraperitoneal injections often resulted in MAP not returning to baseline, but reaching a plateau higher than baseline. The beginning of the plateau was considered as t_{dur} in those cases.

Unpaired, two-tailed, Student's t-tests were conducted between groups to determine statistical significance with $\alpha = 0.05$ when comparison was required.

3.2.5. Bioavailability of Vasopressin

Nine rabbits in this experiment were chosen to receive ^{3}H-radiolabeled vasopressin solutions, three in each of the IV001, IP010 and SQ100 groups. One blood sample was collected before injection as control and up to 7 samples after injection at chosen time points up to 1 hour. Rabbits that received radiolabeled vasopressin were immediately euthanized at the end of the monitoring period with an intravenous injection of sodium pentobarbital.

The drawn blood samples were collected into BD Vacutainer® tubes coated with sodium heparin (VWR, West Chester PA) and immediately refrigerated for further processing. Samples collected within one day were centrifuged at the end of each day to collect plasma. Plasma samples were then solubilized per manufacturer's instructions using SOLVABLE™ (PerkinElmer, Waltham, MA) and counted in a liquid scintillation counter (Packard Tri-Carb 2200CA, PerkinElmer, Waltham, MA) to determine plasma levels.

The bioavailability F of a drug delivered by an experimental route or formulation is expressed by:

$$F = \frac{AUC_{\exp} * Dose_{ref}}{AUC_{ref} * Dose_{\exp}} \quad \text{(Eq. 3.1)}$$

AUC is defined as the area under the plasma concentration versus time curve of the tested drug using the trapezoidal rule, up to the last collected data point [4]. The reference sample is generally an intravenous dose of the drug, as it allows all of the injected drug to be exposed to the body. Each AUC is normalized by the given dose for comparison. The average AUC up to one hour for each group was thus computed to obtain the absolute bioavailability after one hour for IP010 and SQ100.

3.3. Results

3.3.1. Vasopressin Injections

Figure 3.2 shows average ΔMAP plots for each vasopressin group. Placebo groups showed normal fluctuations from their baseline values and are not shown. Rabbits in the IV001 group experienced a sharp spike in MAP within 30 seconds after injection, which immediately subsided. It was then followed by a rapid increase to the peak pressure and rapid decrease back to the baseline. Rabbits in the IP010 and SQ100 groups, in contrast, did not spike and experienced slower rates of increase to their peak MAP and subsequent decrease, as shown in Figures 3.2(b) and 3.2(c), respectively.

Figure 3.3 shows a plot of ΔMAP_{max} vs. t_{max} as reported in Table 3.1 and t_{dur} for all groups, respectively. Rabbits in the IP010 and SQ100 groups experienced significantly higher ΔMAP_{max} ($p < 0.05$) than their respective placebo group. These two groups were also not significantly different from each other for all parameters.

3.3.2. Pharmacokinetics

Figure 3.4 shows average plasma vasopressin levels measured by radiolabeled species in the 3 vasopressin groups. IV001 showed rapid decay of the plasma vasopressin concentration from a nominal initial concentration of 22.2 ± 0.4 ng/mL to 2.9 ± 1.6 ng/mL after 8.7 minutes to a final concentration of 0.7 ± 0.3 ng/mL. The decay did not appear to be exponential, but biphasic. Data in the first 5 minutes suggested a $t_{1/2}$ of 2.2 minutes, and between 5 and 15 minutes, a $t_{1/2}$ of 6.2 minutes. The plasma concentration did not significantly decrease between 30 and 60 minutes.

IP010 initially showed an induction period of 5 minutes or less before increasing to a peak concentration of 8.2 ± 3.7 ng/mL at 30 minutes, then decreased slightly over the next 30 minutes to a final value of 6.5 ± 1.0 ng/mL, which was not significantly different from its peak value. Plasma levels for SQ100 increased linearly in the first 45 minutes at a rate of 0.77 ng/(mL min), after which they increased more slowly to reach a maximum concentration of 37.1 ± 9.2 ng/mL one hour after the injection.

The measured bioavailability of IP010 was found to be 25.0 ± 13.3 % and for SQ100, 10.0 ± 6.3 %.

3.4. Discussion

This work is the first to the author's knowledge to show intraperitoneal and subcutaneous injections of vasopressin at levels that achieved systemic vasoconstriction. The observed behavior of MAP in the different groups is consistent with the initially measured plasma level profiles.

The IV001 group shows an immediate spike in MAP as vasopressin is injected. The origin of the spike is unknown, and has never been reported to the best of the authors' knowledge. One possible explanation is that the response does not pertain to the whole circulatory system, but rather to a local response of the artery where the catheter is introduced, due to aggressive vasoconstriction triggered by a large bolus of vasopressin. Investigation of this phenomenon may yield useful medical data, but is beyond the scope of this research. This instantaneous reaction, however, is likely one of the reasons why vasopressin is typically infused over time in traumatic hemorrhagic shock settings, rather than injected as a bolus. A rapid spike in MAP may dislodge a clot that has formed on a severed blood vessel, and could cause further bleeding before surgical control may be achieved. The rapid elimination of vasopressin from the circulatory system also explains the short duration of effect of an intravenous bolus. King *et al* studied the half-life of an intravenous bolus of vasopressin (52 ng) in anesthetized rabbits and measured a $t_{1/2}$ of 0.9 minutes during the first 5 minutes and a $t_{1/2}$ of 5.4 minutes for the remaining 20 minutes [5]. These values are lower than measured in this work, but the authors also mention differences with other studies based on the anesthetic agent used during experimentation, which could account for the observed difference.

The IP010 and SQ100 groups show a more gradual change in MAP, consistent with the progressive increase in plasma vasopressin shown in the first 15 minutes after injection, at which point the MAP has peaked in both groups. This observed behavior corroborates the concept of a bolus of vasopressin deposited intraperitoneally or subcutaneously and from which vasopressin gradually diffuses into the bloodstream to reach levels where systemic vasoconstriction can be measured. This gradual increase in

vasopressin concentration is more similar to an infusion and would be preferred over an intravenous bolus.

A discrepancy between measured levels and MAP behavior starts beyond 15 minutes after injection. Plasma levels suggest that MAP should remain high (IP010) or increase (SQ100), but it slowly decreases back to baseline values instead. Dworkin *et al* observed the same phenomenon when they investigated vasopressin-induced vasoconstriction in the hepatic vascular bed in rats and found that the vasoconstriction was lost after 15 minutes of a 30-minute vasopressin infusion at ~1.5 μg/kg-min [6]. Their investigation demonstrated that this loss of vasoconstriction was due to the local production of nitric oxide (NO), a vasodilator, which inhibited the action of vasopressin. NO is produced in the vascular endothelium by endothelial nitric oxide synthase (eNOS) in response to elevated intracellular levels of Ca^{2+} in the vascular smooth muscle, which cause vasoconstriction [7]. The produced NO allows the vascular smooth muscle to relax and brings vascular tone back to a normal condition. Long-term inhibition of NO synthesis has further been shown to cause systemic hypertension [7-9]. eNOS is thus an important regulating component of vascular tone. Vasopressin-induced vasoconstriction in healthy rabbits could therefore trigger the regulatory production of NO by eNOS to inhibit the action of vasopressin and maintain a normal vascular tone.

Co-injection of vasopressin with one of the many known NO inhibitors, such as L-NAME (N(G)-nitro-L-arginine methyl ester), would show whether the loss of vasoconstriction observed in this work is due to regulatory NO synthesis. Inhibition by NO may also possibly be avoided in a shock model, since the action of vasopressin would be compensatory rather than a stressor on the vascular system.

It is also noted that the doses used in this study were simply chosen to corroborate pharmacokinetic measurements with a measurable effect on blood pressure and heart rate. They are not necessarily in the therapeutic range, which would have to be determined by a dose-ranging study conducted in a shock model.

The plasma concentration data obtained in this work was not sufficient for an estimation of total bioavailability. Figure 3.4 shows that plasma levels for SQ100 were still rising after one hour, and were not declining significantly for IP010. The real bioavailability for both of these injection routes is thus greater than the calculated values. The obtained values suggest that 25% of the intraperitoneal dose and 10% of the subcutaneous dose had entered the bloodstream after one hour. These numbers agree with the initial assumption that the mesentery, being more vascularized than the subcutaneous site, would allow greater bioavailability. They do not take into account the possible degradation of vasopressin in its injection site, however, because the assay method does not distinguish between whole and degraded vasopressin. They are thus representative of the maximum bioavailability of vasopressin injected intraperitoneally or subcutaneously after one hour.

3.5. Conclusions

This work is the first to report on plasma profiles, effects and bioavailability measured after intraperitoneal and subcutaneous injections of vasopressin in healthy rabbits. The obtained results demonstrate the potential for such injections to achieve prolonged vasoconstriction in shock models. An important implication in the emergency treatment of hemorrhagic shock is the possibility of pre-treating a bleeding trauma patient

with a subcutaneous vasopressin injection before hospital arrival to sustain hemodynamic parameters and delay the onset of shock without the need for catheterization. This method would be especially advantageous in chaotic conditions, where an intravenous catheterization cannot easily be performed.

The candidate locations tested in this work for subsequent implantation of a drug delivery device both showed positive results and potential to release from either site. The intraperitoneal site showed better bioavailability within the first hour, but the surgery needed to implant a device intraperitoneally is currently more invasive than for a subcutaneous implantation. The logistics of implanting devices in all soldiers heading out to military operations theaters, for example, would require a location that is as simple to reach as possible. The subcutaneous location was thus chosen for *in vivo* delivery of vasopressin from the rapid drug delivery device. Further improvements to the device allowing it to be implanted without major surgery (as an injectable device, for example) may make the intraperitoneal location a more attractive site for implantation.

3.6. Figures

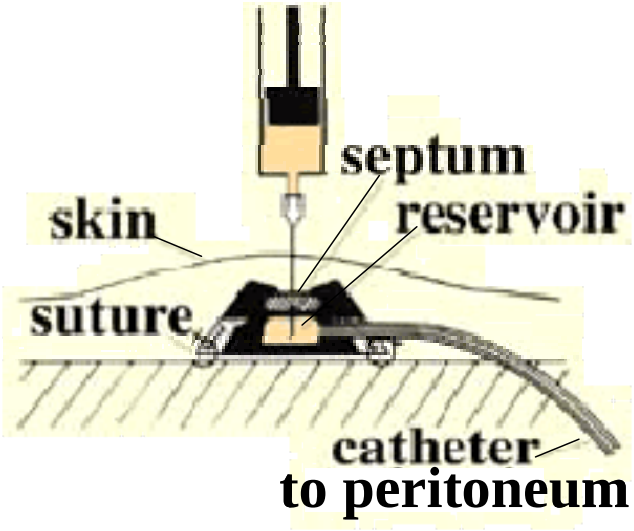

Figure 3.1: Schematic of vascular access port used in intraperitoneal injections.

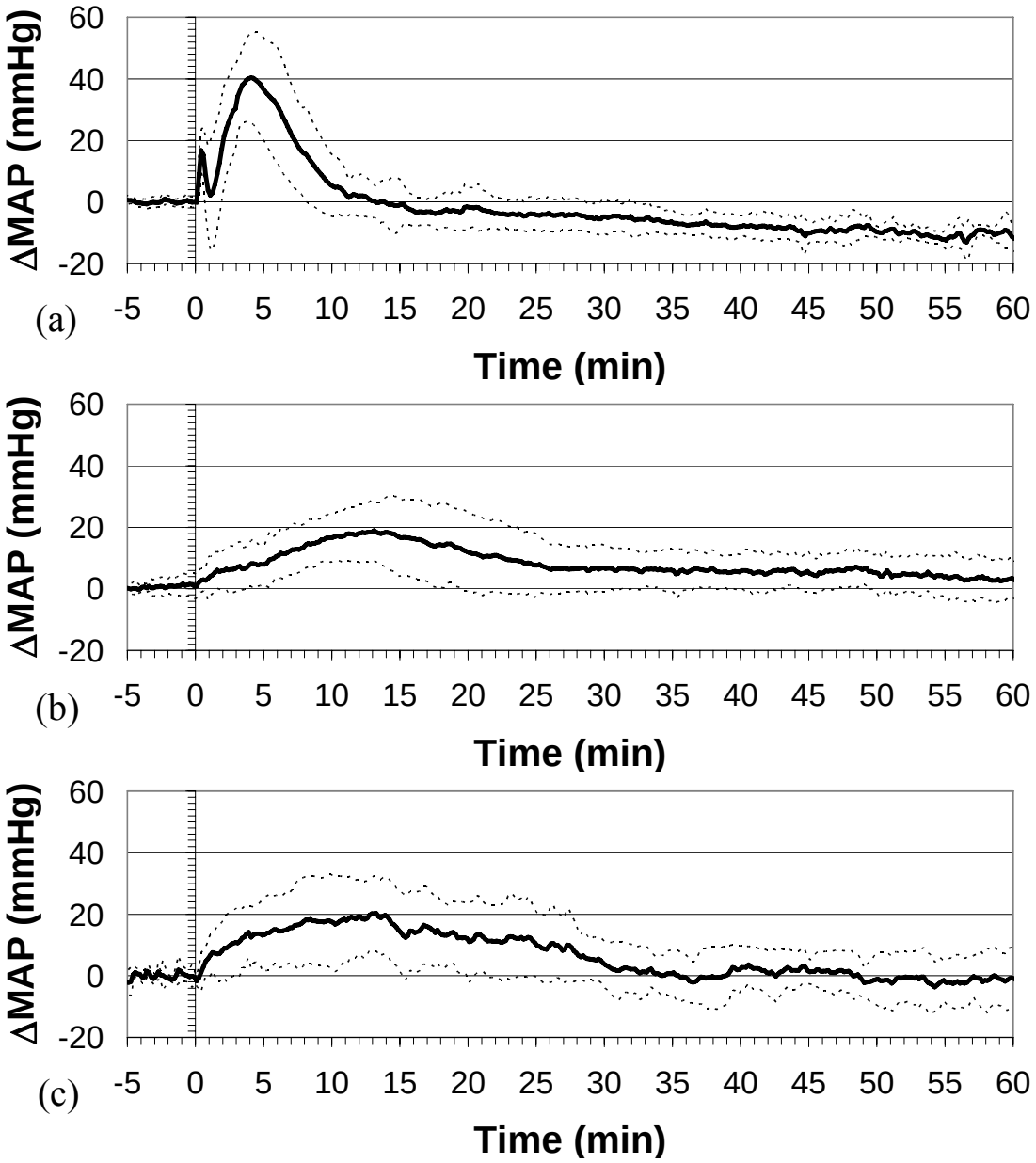

Figure 3.2: Averaged *ΔMAP* profiles after vasopressin injection at t = 0 for groups (a) IV001, (b) IP010 and (c) SQ100. Solid lines are averages of all profiles in the group. Dashed lines represent ± standard deviation.

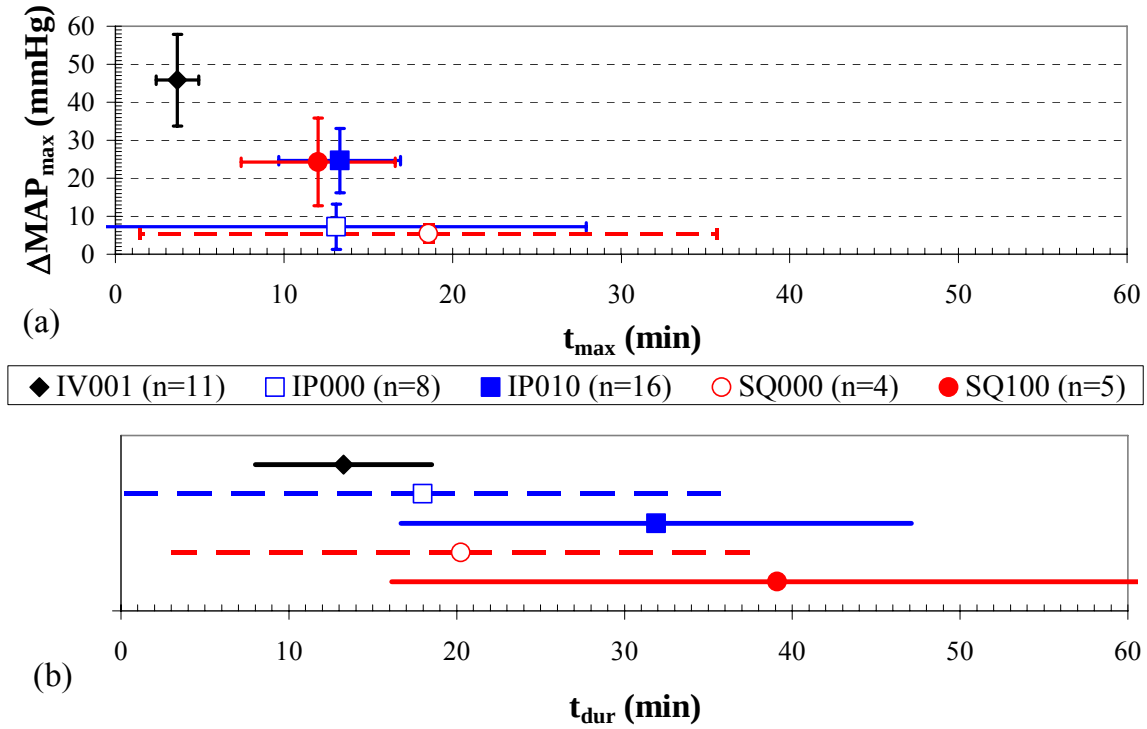

Figure 3.3: Plots of (a) ΔMAP_{max} vs. t_{max} and (b) t_{dur}. Error bars represent standard deviation. The legend is the same for both plots.

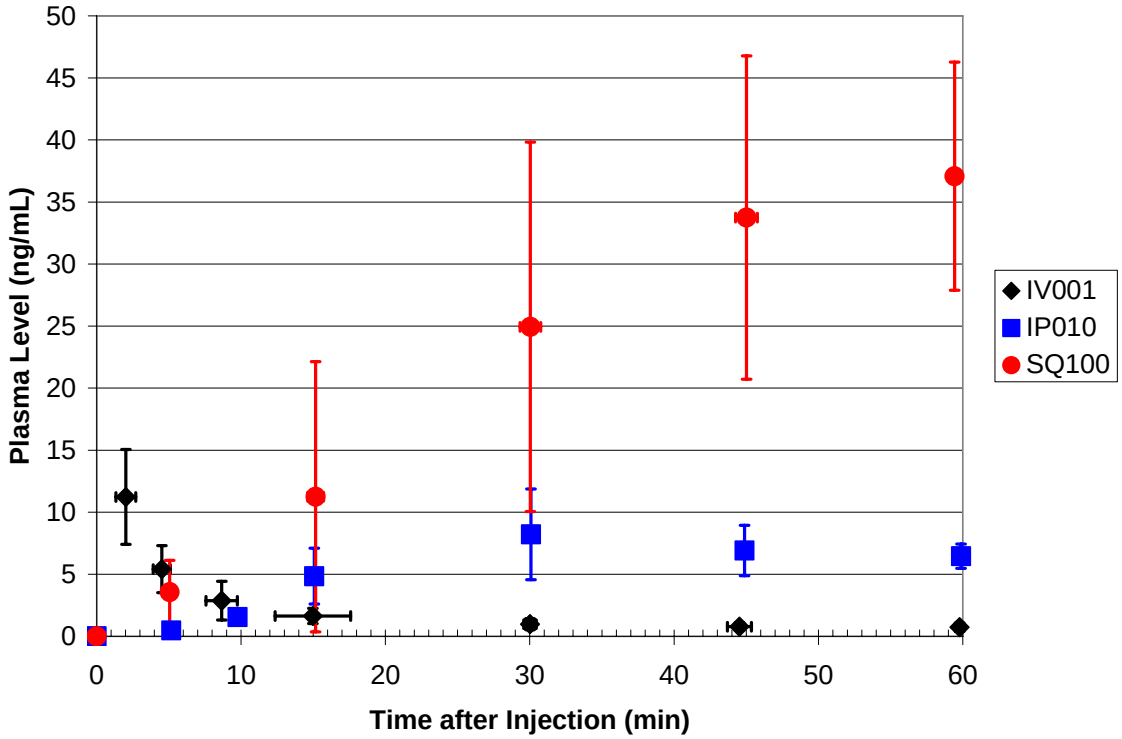

Figure 3.4: Levels of vasopressin as measured by radiolabeled species for the vasopressin groups.

3.7. Tables

Table 3.1: Summary of ΔMAP_{max}, t_{max} and t_{dur} for each test group. Values are reported as mean ± standard deviation.

Group	n	ΔMAP_{max} (mmHg)	t_{max} (min)	t_{dur} (min)
IV001	11	45.8 ± 12.1	3.7 ± 1.3	13.3 ± 5.3
IP000	8	7.2 ± 6.0	13.1 ± 14.8	18.0 ± 18.3
IP010	16	24.6 ± 8.5	13.3 ± 3.6	31.9 ± 15.2
SQ000	4	5.5 ± 2.3	18.6 ± 17.1	20.2 ± 17.1
SQ100	5	24.3 ± 11.5	12.0 ± 4.6	39.1 ± 23.0

3.8. References

1. Teva_Pharmaceuticals, *Desmopressin Acetate Injection: Package Insert*.
2. Rodeghiero, F., G. Castaman, and P.M. Mannucci, *Prospective multicenter study on subcutaneous concentrated desmopressin for home treatment of patients with van Willebrand disease and mild or moderate hemophilia A.* Thrombosis and Haemostasis, 1996. **76**(5): p. 692-696.
3. Mannucci, P.M., *Desmopressin (DDAVP) in the treatment of bleeding disorders: The first 20 years.* Blood, 1997. **90**(7): p. 2515-2521.
4. Chow, S., ed. *Encyclopedia of biopharmaceutical statistics*. 2000, Marcel Dekker: New York, NY.
5. King, K.A., et al., *Pharmacokinetics of Vasopressin and Atrial Natriuretic Peptide in Anesthetized Rabbits.* Endocrinology, 1989. **124**(1): p. 77-83.
6. Dworkin, M.J., P. Carnochan, and T.G. Allenmersh, *Nitric-Oxide Inhibition Sustains Vasopressin-Induced Vasoconstriction.* British Journal of Cancer, 1995. **71**(5): p. 942-944.
7. Alderton, W.K., C.E. Cooper, and R.G. Knowles, *Nitric oxide synthases: structure, function and inhibition.* Biochemical Journal, 2001. **357**: p. 593-615.
8. Qiu, C., et al., *Evolution of Chronic Nitric Oxide Inhibition Hypertension: Relationship to Renal Function.* Hypertension, 1998. **31**(1): p. 21-26.
9. Loichot, C., et al., *Vasopressin Does not Effect Hypertension Caused by Long-Term Nitric Oxide Inhibition.* Hypertension, 2000. **35**(2): p. 602-608.

CHAPTER 4: *IN VIVO* RAPID DELIVERY OF VASOPRESSIN FROM AN IMPLANTABLE DRUG DELIVERY MEMS DEVICE

4.1. Introduction

This chapter reports on the first *in vivo* subcutaneous release of vasopressin from the implantable rapid drug delivery device in a rabbit model, and has been submitted in part for publication to the Journal of Controlled Release. Investigation of intraperitoneal and subcutaneous injections of vasopressin showed measurable effects from both delivery routes. The subcutaneous location was chosen because of the less invasive procedure needed to implant the device. Vasopressin was chosen as a model drug as it is widely used as vasoconstrictor in cardiac arrest [1, 2], and shows promise for use in hemorrhagic shock [3-7]. It is thus a potential candidate for release from the device in this time-sensitive context. Device releases were compared with intravenous and subcutaneous injections of vasopressin to assess bioavailability and compare pharmacokinetics with normal injections. Placebo device releases were also performed to investigate possible effects from the device.

4.2. Materials and Methods

4.2.1. Vasopressin

Arginine vasopressin acetate powder (Sigma-Aldrich, Saint-Louis, MO) was reconstituted with sterile water to appropriate concentration for injection or device loading. ^{3}H-radiolabeled vasopressin (American Radiolabeled Chemicals, St. Louis, MO) was added to injection solutions for determination of plasma levels of vasopressin.

4.2.2. Devices

Device fabrication and drug loading have been extensively described in Chapter 2. Three devices were filled with 20 μL of radiolabeled solution containing a vasopressin dose of 100 μg/kg and 4 devices were filled with 20 μL of sterile water.

4.2.3. Animal Study

This study was approved by MIT's Committee on Animal Care and the Animal Care and Use Review Office from the Department of Defense Medical Research and Material Command. Nineteen male New Zealand White rabbits with weights between 2.5 kg and 3.5 kg were obtained (Covance Research Products, PA, USA). The animals were housed in compliance with MIT's Committee on Animal Care husbandry guidelines, with unrestricted access to water and food.

Rabbits were anesthetized with an initial dose of midazolam (2 mg/kg, IV) and were maintained under anesthesia by mask with 1-3% isoflurane in balance oxygen. One ear was catheterized for intravenous access, while the central auricular arteries in both

ears were catheterized for mean arterial pressure (MAP) monitoring and blood sampling, respectively.

Rabbits received 1 μg/kg vasopressin intravenously (IV001 group, n = 11), 100 μg/kg subcutaneously (SQ100 group, n = 5), or were implanted with a device containing 100 μg/kg vasopressin (DV100 group, n = 3) or sterile water (DV000 group, n = 4). Implanted devices were introduced through a skin incision on the left foreleg and placed subcutaneously over the tricep, with the drug exit side facing the muscle. Biocompatible Teflon-sheathed electrical leads were used to connect the microheaters to the external power source through the incision. Devices were activated by applying 9V to the microheaters for 10 seconds, followed by a 15 second pause and ten 5-second applications of 9V with 5-second intervals, in order to minimize heat exposure to the animal and drug degradation due to activations. Rabbits were monitored for 1 hour following injection or activation then euthanized by sodium pentobarbital injection. Four of the rabbits from the IV001 group were allowed to wake up from anesthesia, left to recover for 7 to 14 days then received another IV injection before being euthanized.

MAP was monitored and recorded continuously by direct blood pressure measurement from an arterial catheter in the central auricular artery, using a Blood Pressure Analyzer^{TM} 400 with DMSI software (Micro-Med, Louisville, KY). Values were measured every 0.5 seconds and averaged over 10 seconds to yield a single data point.

ΔMAP was defined as the difference between MAP and baseline MAP, which is the average MAP measured over 5 minutes before injection. *ΔMAP* plots for each injection were subsequently analyzed (Excel 2003, Microsoft, Inc., USA) to extract the

maximum ΔMAP (ΔMAP_{max}), the time needed to reach that maximum (t_{max}), and the time at which ΔMAP returned under baseline level for at least 1 minute thereafter (t_{dur}).

Unpaired, two-tailed, Student's t-tests were conducted between groups to determine statistical significance with α (significance level) = 0.05 when needed.

4.2.4. Plasma Levels of Vasopressin

Nine rabbits in this experiment were chosen to receive ^{3}H-radiolabeled vasopressin solutions, three in each of the IV001, SQ100 and DV100 groups. One blood sample was collected before injection as control and up to 7 samples after injection at chosen time points up to 1 hour. Rabbits that received radiolabeled vasopressin were immediately euthanized at the end of the monitoring period with an intravenous injection of sodium pentobarbital.

The drawn blood samples were collected into BD Vacutainer® tubes coated with sodium heparin (VWR, West Chester PA) and immediately refrigerated for further processing. Samples collected within one day were centrifuged at the end of each day to collect plasma. Plasma samples were then solubilized per the manufacturer's instructions using SOLVABLE™ (PerkinElmer, Waltham, MA) and counted in a liquid scintillation counter (Packard Tri-Carb 2200CA, PerkinElmer, Waltham, MA) to determine plasma levels.

The bioavailability F of a drug delivered by an experimental route or formulation is expressed by:

$$F = \frac{AUC_{\exp} * Dose_{ref}}{AUC_{ref} * Dose_{\exp}} \qquad \text{(Eq. 3.1)}$$

AUC is defined as the area under the plasma concentration versus time curve of the tested drug using the trapezoidal rule, up to the last collected data point [8]. The reference sample is generally an intravenous dose of the drug, as it allows for all of the injected drug to be exposed to the body. Each AUC value is normalized by the given dose for comparison. The average AUC up to one hour for each group was thus computed to obtain the absolute bioavailability after one hour for DV100 and SQ100.

4.3. Results

4.3.1. Vasopressin Delivery

Figure 4.1 shows averaged ΔMAP profiles for all groups, while Table 4.1 summarizes data analysis results. Figure 4.1(a) shows the results for intravenous injections (IV001 group), demonstrating a sharp spike in MAP within 30 seconds after injection that immediately subsides. It was then followed by a rapid increase to the peak pressure and rapid decrease back to the baseline. Figure 4.1(b) shows the results for subcutaneous injections (SQ100 group), which, in contrast to subcutaneous injections, rose at a slower rate to a maximum peak then returned to baseline after almost 40 minutes. Figure 4.1(c) shows the results for the implanted microdevices (DV100 group), which exhibited a combination of both the intravenous and subcutaneous delivery modalities. The MAP reached a maximum peak significantly different from placebo in a time similar to an intravenous injection, but slowly returned to baseline after approximately 33 minutes, similarly to a subcutaneous injection. It also shows a slight dip in MAP within the first 2 minutes. Figure 4.1(d) represents the results for the placebo device (DV000

group), which showed the same dip within the first 2 minutes, but no other notable feature.

4.3.2. Pharmacokinetics

Figure 4.2 shows measured plasma levels in the three groups that received vasopressin. IV001 showed rapid decay of the plasma vasopressin concentration from an estimated initial concentration of 22.2 ± 0.4 ng/mL to a final concentration of 0.7 ± 0.3 ng/mL. A bi-phasic exponential decay was measured with a $t_{1/2}$ of 2.2 minutes in the first 5 minutes, and a $t_{1/2}$ of 6.2 minutes between 5 and 15 minutes. The plasma concentration did not significantly decrease between 30 and 60 minutes. Plasma levels for SQ100 increased linearly in the first 45 minutes at a rate of 0.77 ng/(mL min), after which they increased more slowly to reach a maximum concentration of 37.1 ± 9.2 ng/mL one hour after the injection. Plasma levels in DV100 animals initially rose to 5.1 ± 1.3 ng/mL after 3.6 minutes, but increased at a slower rate of 0.35 ng/(mL min) thereafter to reach a final concentration of 24.4 ± 2.9 ng/mL after one hour.

The bioavailability of DV100 was calculated to be greater than 6.2 ± 2.8 % and for SQ100, greater than 10.0 ± 6.3 %, for the same reasons outlined in the previous chapter.

4.4. Discussion

This work has shown that a MEMS drug delivery device implanted subcutaneously was able to deliver a dose of vasopressin capable of showing a measurable effect on blood pressure in healthy rabbits. Peak effect was achieved within

5 minutes and lasted approximately 30 minutes. Results suggest that vasopressin quickly entered the circulatory system causing an increase in MAP as early as 2 minutes after the start of activation. The similar behavior observed following a subcutaneous injection and the measured pharmacokinetic profile both support that this MAP increase was due to the release of vasopressin. The release of vasopressin from a device results in a rapid onset effect with relatively long duration, potentially making the device superior to both intravenous and subcutaneous injections in terms of therapeutic efficacy. Testing of the device in a shock model will provide the definitive answer.

The bioavailability of vasopressin released from the device was found to be lower than that from a subcutaneous injection of the same dose. This reduced bioavailability may be due to incomplete release from the device or the difference in volume and concentration of vasopressin administered via each delivery route, which may vary the entrance rate of vasopressin. It is to be noted, however, that the standard deviation of the device results is much smaller than that of the subcutaneous injections, be it in the ΔMAP profile or plasma levels. A drug delivered from the device may be able to reach more consistent pharmacokinetics than simple injections. Increased sample size for device release of vasopressin is needed to confirm this.

The power applied during activation of the device was cycled because of concern that the thermal energy released by the device may degrade vasopressin. The cycling of power did not significantly degrade the vasopressin, but the released thermal energy may have slightly affected the animals. A small dip in MAP was observed during activation of the loaded and placebo devices. Reduction of the thermal energy released to the

environment by better insulation is an objective for improvement of future generations of the device.

The extended duration of effect achieved by subcutaneous injection and device release of vasopressin correlates with initial plasma levels, but at times beyond the peak pressure, this effect is progressively lost, despite the continually increasing plasma levels. The observed discrepancy between blood pressure and plasma level is similar to that observed by Dworkin *et al*, who reported a loss of vasoconstriction after 15 minutes of a 30-minute infusion of vasopressin directly to the hepatic arterial bed in rats [9]. Their work demonstrated that this loss of vasoconstriction was tied to the triggered production of nitric oxide (NO), which caused vasodilation. It is conceivable that the injection of vasopressin in a healthy animal is seen as a stressor, thus triggering a regulatory mechanism through NO synthesis to bring the blood pressure back to normal levels. A device release of vasopressin in a hemorrhagic shock model may therefore show a more extended effect than seen in this work, because the vasoconstriction would be compensatory, rather than a stressor.

An alternative explanation for the loss of vasoconstriction is the degradation of vasopressin over time, either in the blood or before entering the bloodstream, although it has been shown not to degrade in rat serum *in vitro* for up to 8 hours [10]. Injection or release of vasopressin in the presence of a NO inhibitor such as L-NAME (N(G)-nitro-L-arginine methyl ester) should tip the scale toward one of these hypotheses, depending on whether it prolongs vasoconstriction in healthy animals.

Another point to address if this device is to be used in a hemorrhagic shock model is that in such models the peripheral circulation is already reduced due to reduced blood

volume and vasoconstriction of the peripheral arterioles. Total peripheral vascular resistance is increased in this situation and may hamper the pharmacokinetics of vasopressin. The increasing plasma levels of vasopressin seen in this work despite vasoconstriction suggest that this may not be a problem, although the reduced blood volume may play a role in shock. This issue is only valid in a hemorrhagic shock model. Other conditions where peripheral circulation is not affected would not encounter such issues.

This work did not address the issues of long-term implantation, where the formation of a fibrous capsule around the device may prevent diffusion of vasopressin. Work by Prescott *et al*, however, has shown that this capsule does not affect the pharmacokinetics of leuprolide, another polypeptide with similar molecular weight to vasopressin [11]. Vasopressin could be similarly unaffected, but investigation of the effect of the fibrous capsule on the diffusion of vasopressin will be required to confirm the viability of the device for long-term use. Long-term implantation would also affect the stability of vasopressin in solution. A dual-chamber concept for the device is being investigated for that purpose, where the drug would be kept in a lyophilized form in one chamber. The drug would be rapidly reconstituted and released with media kept in a separate chamber upon activation.

4.5. Conclusions

This work is the first to demonstrate the *in vivo* delivery of vasopressin from a MEMS drug delivery device producing a measurable effect on blood pressure in rabbits. The results obtained in this work warrant further investigation of the device in a

hemorrhagic shock model. Further research is required to address issues associated with long-term implantation. Its application could extend beyond vasopressin to address acute conditions treatable with other drugs, such as atropine or epinephrine.

4.6. Figures

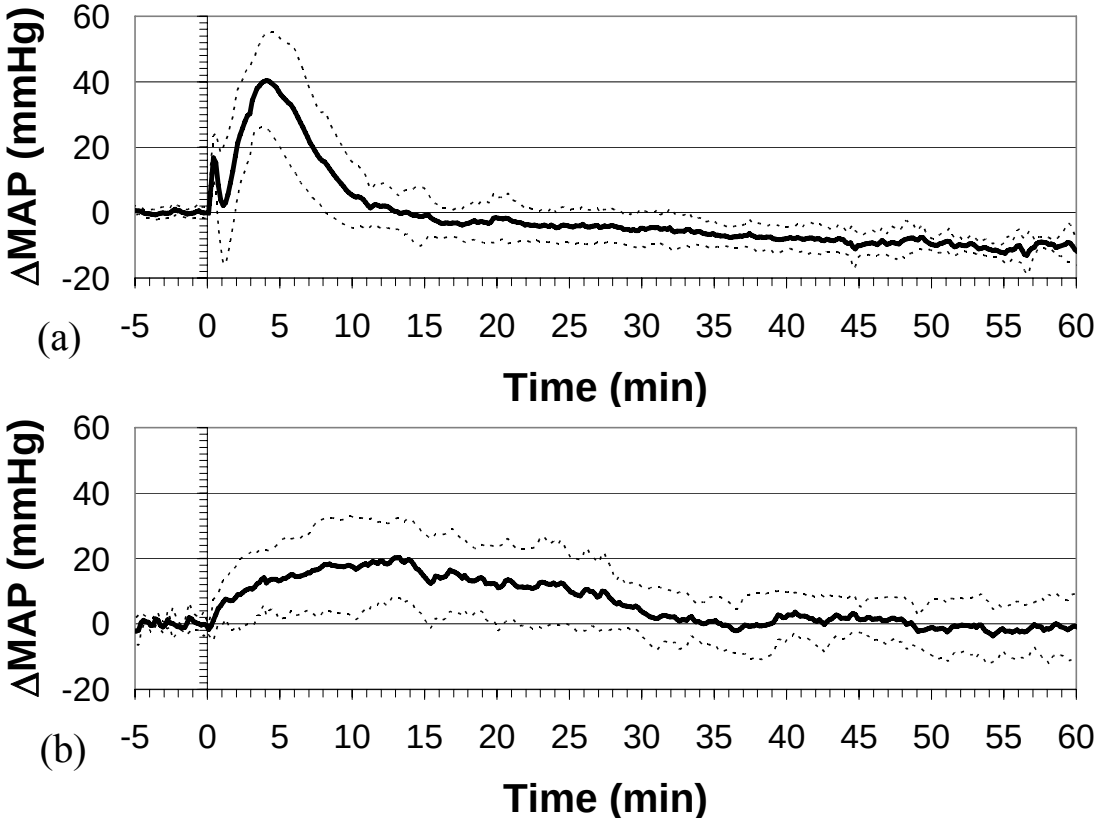

Figure 4.1: Average *ΔMAP* profile for groups (a) IV001, (b) SQ100. Dashed lines represent ± standard deviation.

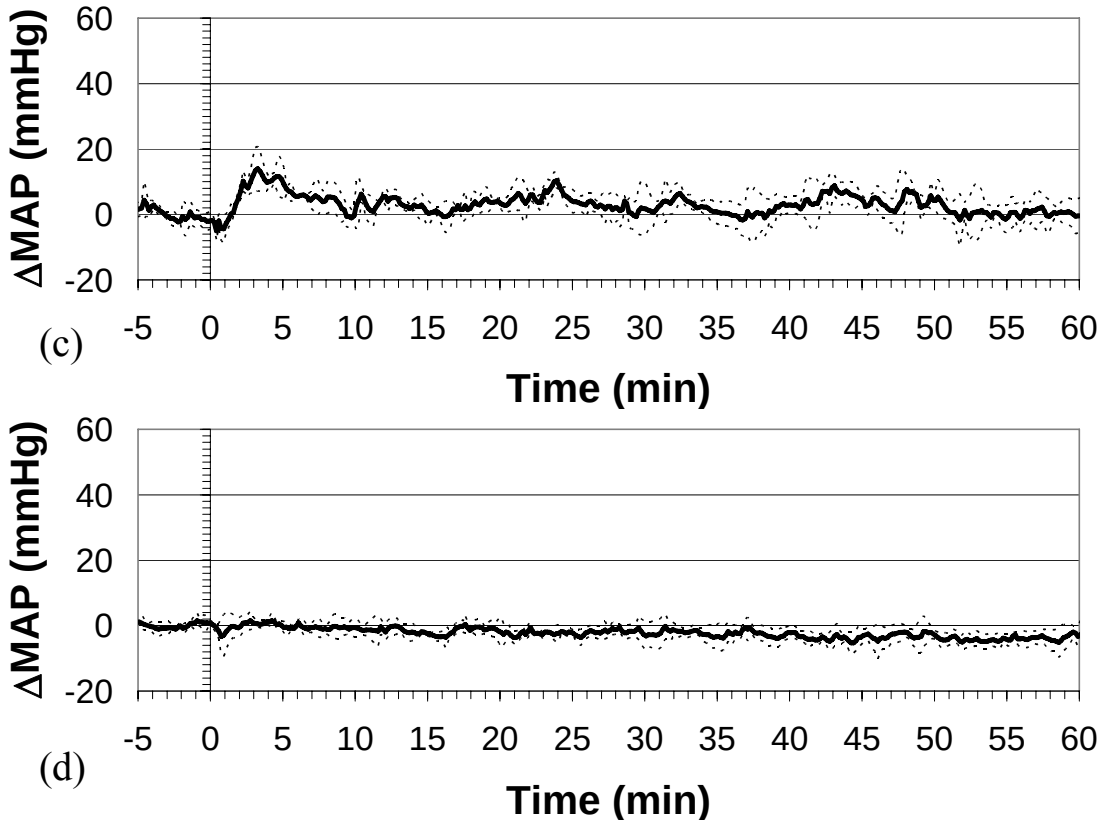

Figure 4.1: Average *ΔMAP* profile for groups (c) DV100 and (d) DV000. Dashed lines represent ± standard deviation.

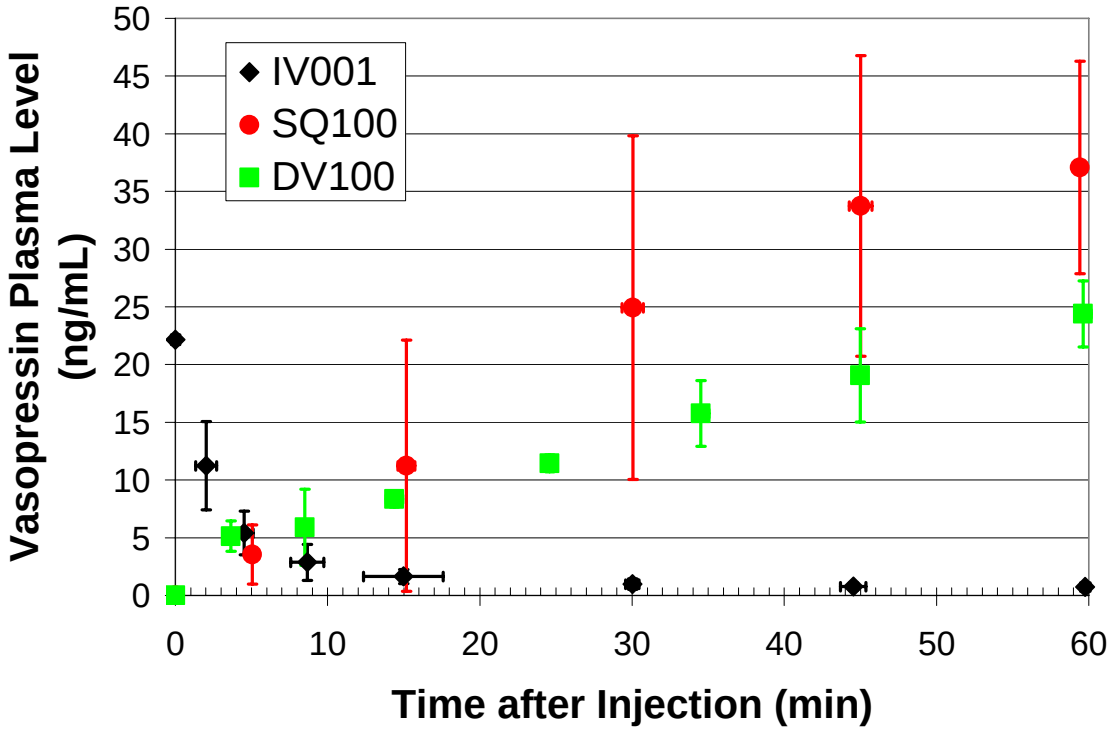

Figure 4.2: Vasopressin plasma levels measured by liquid scintillation counting

4.7. Tables

Table 4.1: Summary of ΔMAP_{max}, t_{max} and t_{dur} for each test group. Values are reported as mean ± s.d. p-values are results of student-t tests compared with DV100.

Group	ΔMAP_{max} (mmHg)	p	t_{max} (min)	p	t_{dur} (min)	p
IV001	45.8 ± 12.1	< 0.05	3.7 ± 1.3	0.61	13.3 ± 5.3	< 0.05
SQ100	24.3 ± 11.5	0.26	12.0 ± 4.6	< 0.05	39.1 ± 23.0	0.65
DV100	17.2 ± 4.2	---	4.0 ± 0.9	---	33.9 ± 6.0	---
DV000	4.7 ± 0.7	< 0.05	15.7 ± 22.6	---	18.0 ± 21.6	---

4.8. References

1. *2005 American Heart Association Guidelines for Cardiopulmonary Resuscitation and Emergency Cardiovascular Care - Part 7.2: Management of Cardiac Arrest.* Circulation, 2005. **112**(24_suppl): p. IV-58-66.
2. Wenzel, V., et al., *A Comparison of Vasopressin and Epinephrine for Out-of-Hospital Cardiopulmonary Resuscitation.* N Engl J Med, 2004. **350**(2): p. 105-113.
3. Raedler, C., et al., *Treatment of Uncontrolled Hemorrhagic Shock After Liver Trauma: Fatal Effects of Fluid Resuscitation Versus Improved Outcome After Vasopressin.* Anesth Analg, 2004. **98**(6): p. 1759-1766.
4. Tsuneyoshi, I., et al., *Low-dose vasopressin infusion in patients with severe vasodilatory hypotension after prolonged hemorrhage during general anesthesia.* Journal of Anesthesia, 2005. **19**(2): p. 170-173.
5. Krismer, A.C., et al., *Employing vasopressin as an adjunct vasopressor in uncontrolled traumatic hemorrhagic shock - Three cases and a brief analysis of the literature.* Anaesthesist, 2005. **54**(3): p. 220-224.
6. Sharma, R.M. and R. Setlur, *Vasopressin in hemorrhagic shock.* Anesthesia and Analgesia, 2005. **101**(3): p. 833-834.
7. Wenzel, V., *Vasopressin in Traumatic Hemorrhagic Shock Study*. 2009, ClinialTrials.gov.
8. Chow, S., ed. *Encyclopedia of biopharmaceutical statistics*. 2000, Marcel Dekker: New York, NY.
9. Dworkin, M.J., P. Carnochan, and T.G. Allenmersh, *Nitric-Oxide Inhibition Sustains Vasopressin-Induced Vasoconstriction.* British Journal of Cancer, 1995. **71**(5): p. 942-944.
10. Grzonka, Z., et al., *In vitro degradation of some arginine-vasopressin analogs by homogenates of rat kidney, liver and serum.* Peptide Research, 1991. **4**(5): p. 270-274.
11. Prescott, J.H., et al., *Chronic, programmed polypeptide delivery from an implanted, multireservoir microchip device.* Nature Biotechnology, 2006. **24**(4): p. 437-438.

CHAPTER 5: TELEMETRIC ACTIVATION AND RAPID RECONSTITUTION

5.1. Introduction

Two of the requirements delineated in Chapter 1 for an implantable emergency drug delivery device are long-term stability of the drug and the ability for telemetric activation, since the time until the device is needed is unknown, but activation must be available immediately at the push of a button if no sensors are integrated with the device for a closed-loop system. This chapter presents proof-of-concept experiments conducted for the requirements of the device developed in this work.

5.2. Rapid Reconstitution Device

5.2.1. Introduction

Drugs in aqueous solutions are seldom stable for long periods of time due to hydrolization. Vasopressin retains at least 95% of its intact form for only 3 days in water at 37°C, for example. Many drugs are stored in lyophilized form, due to the solid phase being more stable, which also allows them to withstand higher temperatures. This feature is desirable for an implanted drug delivery device with unknown time to activation. The requirement for rapid drug delivery, however, does not allow the drug to remain in solid form when the device is activated, since diffusion by itself would not allow rapid delivery.

One solution to the problem would be to physically expel the lyophilized drug from the device, although this solution would require a moving component, which is not

always reliable. Another concept, presented in this work, is a dual-reservoir design for the drug delivery device. The original device as presented in this work is first filled with reconstitution media. An additional Pyrex reservoir containing the lyophilized drug is appended to the device and is capped by a second membrane chip. The reservoirs are thus hermetically separated by a silicon nitride membrane chip. Activation of the device breaks the intermediate membrane and expels the liquid into the drug, reconstituting it then further forcing the solution out of the device.

5.2.2. Experimental Method

A proof-of-concept experiment was conducted on one device. The first reservoir was loaded with 20 μL of water and sealed as previously described. The second reservoir was then loaded with 4 mg of atropine sulfate (Sigma-Aldrich, Inc., St. Louis, MO), a drug used as an anti-nerve gas agent. The reservoir was covered with a waterproof adhesive tape to allow filming of the reconstitution event inside the second reservoir, and the tape was slit with a razor blade to allow fluids to escape. Figure 5.1 shows the device before activation. The device was placed under a stereoscope fitted with a digital camera to record the event. A voltage of 9 V was applied to the microresistors of the device for 25 seconds then removed.

5.2.3. Results

Figure 5.2 shows frames of the reconstitution event captured by the camera. The device is activated at $t = 0$ s (Figure 5.2(a)). The intermediate membrane breaks at $t = 8.233$ s, represented in Figure 5.2(b) and evidenced in the video by a sudden shift in

the atropine. The difference is not obvious with a still image. Darkening of the powder shown in Figure 5.2(c) at t = 12.067 s signals the diffusion of water up to the upper layers of the atropine reservoir. Fluid starts exiting the slit in the tape immediately afterwards, shown in Figure 5.2(d). The amount of fluid exiting the device increases steadily from there onwards, as shown in Figures 5.2(e) and 5.2(f). The activation is terminated at t = 25 s.

5.2.4. Discussion

This experiment indicates that rapid reconstitution and release from an implantable device may be possible, although the amount of drug expelled from the device was not quantified. One approach to increase reconstitution and release yield is using a smaller powder chamber. This configuration will decrease the amount of space between powder particles and will allow the liquid to come in contact with all of the powder more easily. Another approach is to force the liquid to move through all of the contained powder before being able to exit the device. This approach would allow maximum interaction between the liquid and powder for reconstitution and expulsion of the drug.

5.3. Telemetric Activation

5.3.1. Introduction

Implantable biomedical devices are developed for the purpose of surpassing current diagnostic or treatment limitations. The drug delivery device developed in this work, for example, aims to allow rapid drug delivery in situations when it may not be

possible otherwise. Interfacing of this device with *in vivo* sensors developed by other researchers could lead to a closed-loop system able to detect and automatically handle an emergency. There may be cases where *in vivo* sensors may not detect the emergence of symptoms or do not exist for the symptoms to be detected, however, and a wireless, manual control would be required to activate the drug delivery device.

This section presents a proof-of-concept for wireless activation of the device with power supplied by 9V batteries in a military scenario of remote casualty search and treatment. This experiment was conducted in collaboration with Prof. Bordetsky from the Naval Postgraduate School, Monterey, CA at the Camp Roberts military camp in California.

5.3.2. Experimental Method

Three devices were loaded with 20 μL of a solution of 1 mg/mL methylene blue (Sigma-Aldrich, Inc., St. Louis, MO) as previously described. Three controls of 20 μL were also injected into square plastic cuvettes with 3 mL of deionized (DI) water. Devices were placed inside similar cuvettes containing 3 mL DI water, with Teflon-sheathed electrical leads extending through the cuvette lids. Each device was connected to a control system linked to a Blackberry phone to receive the activation signal, as shown in Figure 5.3. The control system included a signal transducer to transform an auditory signal of 1 kHz relayed by the Blackberry to an "ON" state for a switch that closed the circuit to which the device was connected. Power for the control system and device was provided by four 9 V batteries connected in parallel.

Each device was activated for 45 seconds in a separate cuvette, after which the device was removed and absorption at 668 nm was measured from each cuvette using a UV-vis absorption spectrometer. Each control was also measured with serial dilutions to obtain a calibration curve, which was used to quantify the amount of solution released from each device. The calibration curve was linear with concentration (not shown).

5.3.3. Results

Measurements obtained from the three devices revealed that 84.6 ± 2.1 % of the loading was released when activated wirelessly and powered by 9V batteries.

5.3.4. Discussion

This work has provided proof-of-concept for the wireless activation of the drug delivery device developed in this work. Quantification of the release with methylene blue revealed that devices connected to 9V batteries released a smaller fraction of their loading than devices connected to a stable power supply (84.6% vs. 92.9%, respectively). This result is expected, since the batteries are not expected to sustain the same voltage as a power supply while being drained continuously for 45 seconds. Starting and ending voltages were measured for 5 other devices previously activated in the same fashion (not shown). The starting voltage was measured to be 8.24 ± 0.11 V and the average voltage drop after 45 seconds of current application was 0.24 ± 0.04 V. The smaller voltage applied to the devices thus explains the reduced release volume because of reduced power output. No quantitative comparisons could be made, however, because current was not recorded as a function of time.

The results obtained in this study, while providing proof of concept, highlight one of the major deficiencies of the current device. The current and power consumption of the device are very high for a device to be implanted with a limited power supply. Four standard 9V batteries were needed to provide enough current to the device for operation. Ultra-high density capacitors may be able to deliver enough current to the device, but it is expected that these capacitors would lack the capacity to sustain activation for 45 seconds. The greatest improvements needed for future generations of this device are in reducing heat losses to the surroundings. This will improve device performance on all fronts, from duration of activation to total current and power consumed, and will thus allow the device to function within more realistic constraints. Other modes of drug expulsion which do not produce heat might also be considered, but they either rely on moving parts which have lower reliability (e.g., micro-pumps) or on electrochemical reactions which have shown lesser reproducibility.

5.4. Conclusions

The results obtained from the experiments presented in this chapter have provided complementary proof-of-concept to the rapid drug delivery device developed in this research, towards a realistic system. They have opened a new avenue of research in the use of this device for rapidly reconstituting drugs, and highlight the need for improving device performance through reduction of heat losses. Alternate systems may be considered, but may result in lower reliability or reproducibility.

5.5. Figures

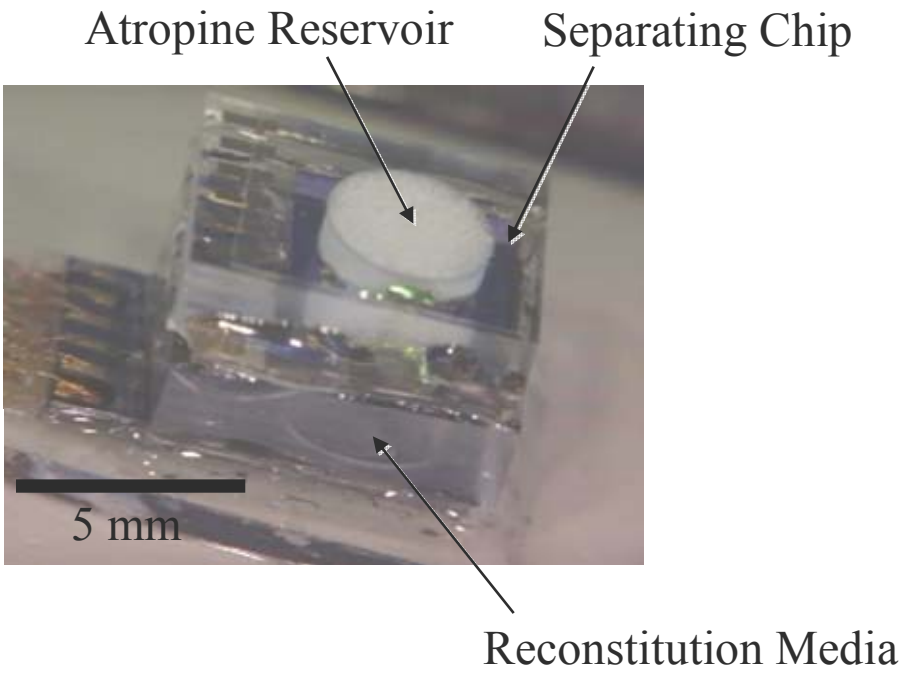

Figure 5.1: Picture of assembled rapid reconstitution device.

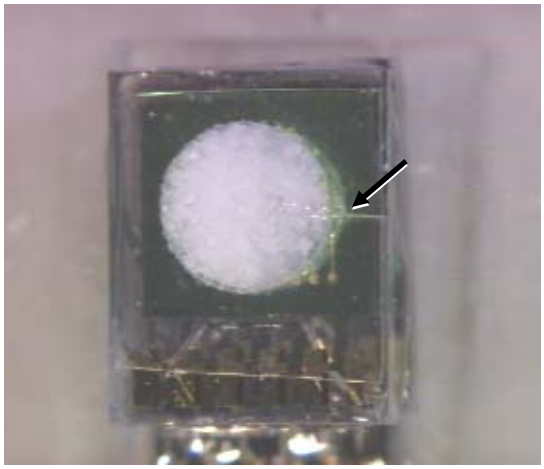

(a) t = 0.000 sec

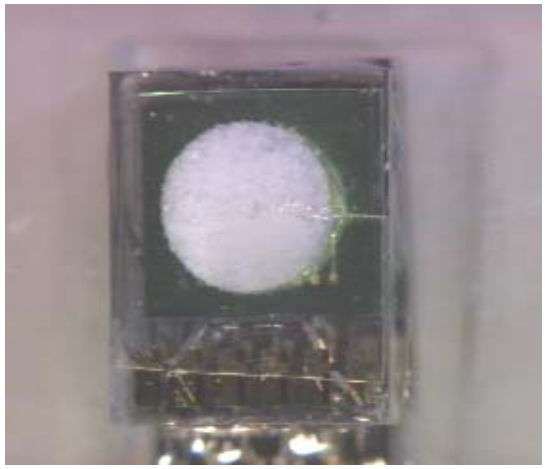

(b) t = 8.233 sec

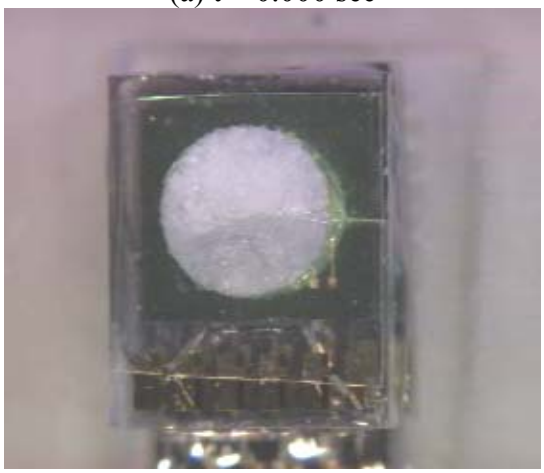

(c) t = 12.067 sec

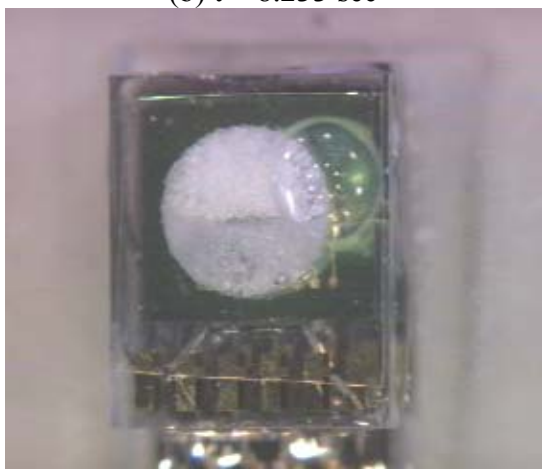

(d) t = 12.567 sec

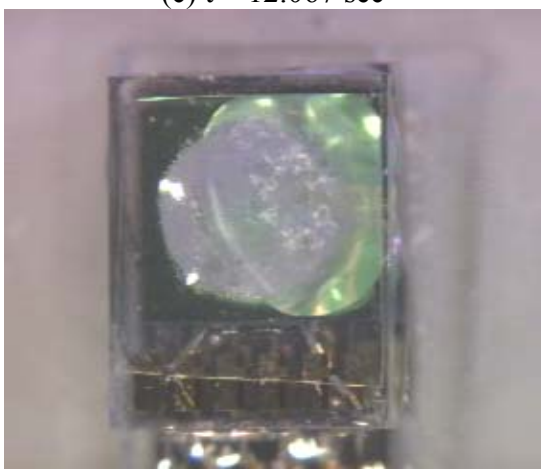

(e) t = 15.000 sec

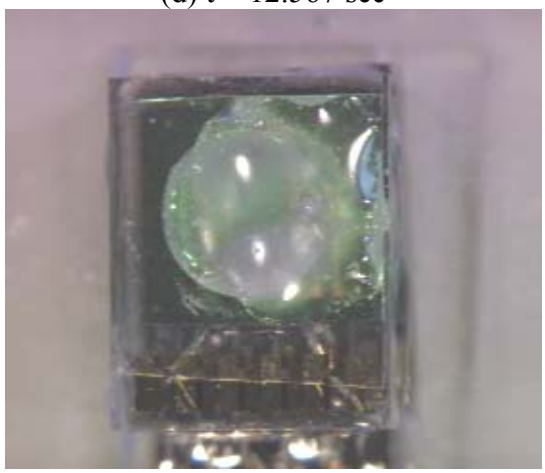

(f) t = 25.000 sec

Figure 5.2: Image capture of rapid reconstitution experiment. Times indicated are with respect to the start of activation. The arrow indicates the slit that allows fluids to escape.

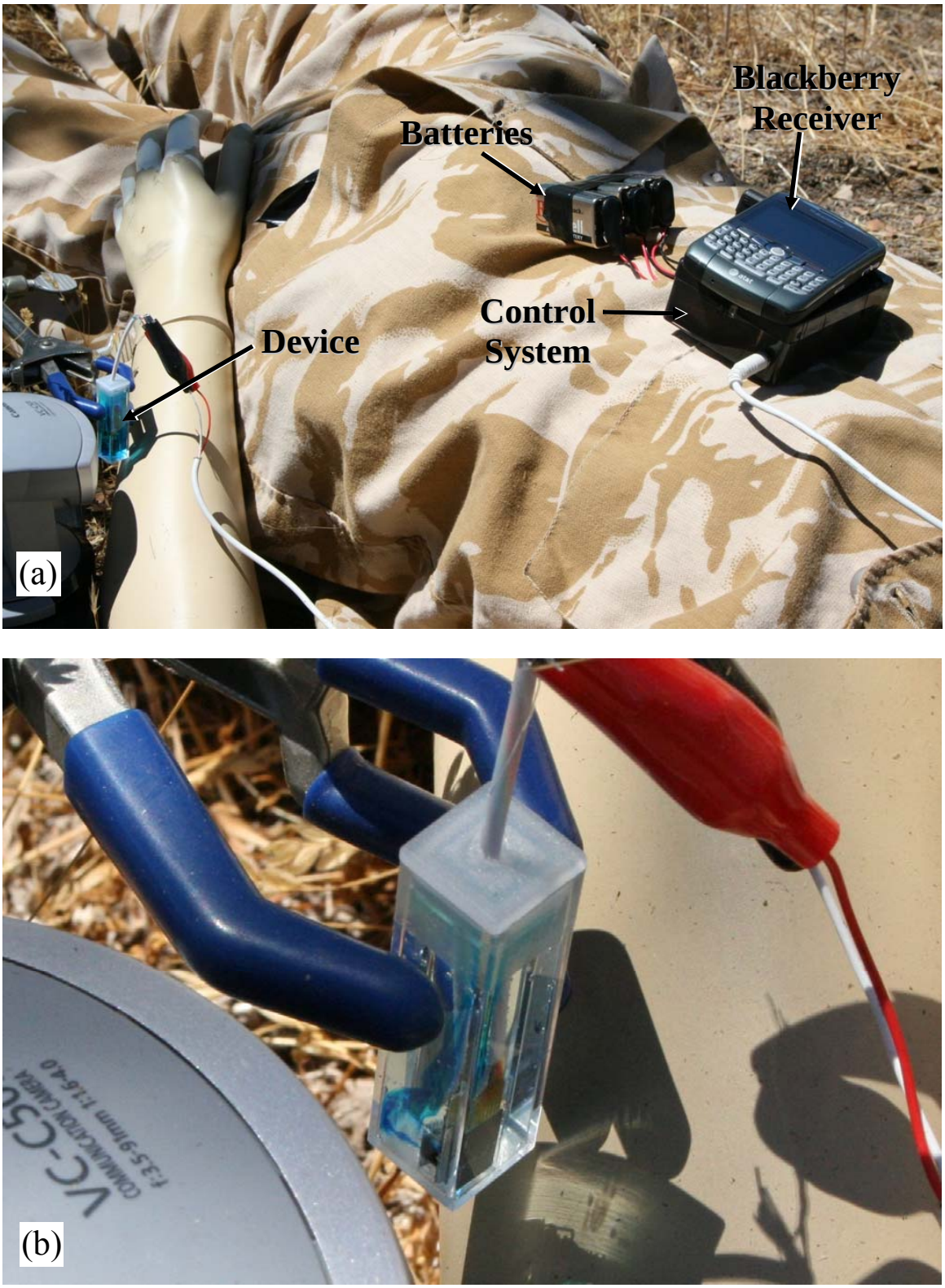

Figure 5.3: (a) Picture of wireless activation control system. The system was placed on a mannequin to simulate a wounded soldier in the military search-and-rescue scenario including the activation of the devices. (b) Picture of device during wireless activation.

CHAPTER 6: SUMMARY AND FUTURE OPPORTUNITIES

6.1. Summary

The first implementation of a rapid drug delivery device for emergency therapy has been demonstrated in this work, culminating with the release of vasopressin in rabbits. The device was fabricated using MEMS technology and presents a modular architecture allowing customization of each part. Its operation is based on the nucleation of vapor bubbles inside the drug reservoir by heated micro-resistors to expel the drug solution. *In vitro* characterization of the device showed reliable and reproducible vasopressin release with limited degradation for an applied potential of 9 V for 45 seconds.

Intraperitoneal and subcutaneous implantation locations were investigated. The subcutaneous location, despite needing approximately 100 times the intravenous dose to show a measurable effect, was chosen because of the less invasive nature of implantation.

The device was implanted subcutaneously in rabbits with a pre-determined dose and activated. Effects of the released drug were monitored by continuous blood pressure measurements. Plasma levels of vasopressin as a function of time were also measured by liquid scintillation counting of plasma samples to detect radiolabeled vasopressin mixed with the release solution. The bioavailability of vasopressin delivered by the device one hour after activation was calculated from plasma level measurements to be 6.2%. This experiment demonstrated the potential of the developed device to deliver drugs in a timely manner in emergency therapies.

Additional proof-of-concept experiments were conducted with the device. A dual-chamber design with the device as a base was used to demonstrate the possibility for

rapid reconstitution and delivery of a lyophilized drug. A battery-powered, wireless control system was also implemented to achieve remote activation of the device.

6.2. Future Opportunities

6.2.1. Device Development

The first generation of the device managed to establish the possibility for rapid and reliable *in vivo* drug delivery from an implantable device, but its power production and current requirement were too high to be easily implemented for real-life use. Another concern came from the heat dissipated to the surroundings of the device during activation that may damage biological tissues. A final concern was that the duration of activation resulted in large energy consumption, which current capacitors or batteries could not supply while sustaining the current needed by the micro-resistors during activation.

All of these problems can be addressed by redesigning the device to reduce heat loss. Reduction of heat loss will lead to lower power requirements, less potential tissue damage and shorter activations. The heat produced by the micro-resistors will predominantly produce vapor bubbles rather than be conducted away by the substrate. Alternative heatless means of expelling the liquid from the device could also be explored, although reliability and reproducibility of these means will have to be determined and compared to the current mechanism.

An interesting avenue for future research is the dual-chamber concept for rapid reconstitution that was summarily demonstrated. Successful implementation of this system could address long-term stability of drugs in the device. The remaining issue

regarding the long-term implantation device is the effect of the fibrous capsule, which would inevitably form around the implanted device, on the pharmacokinetics of vasopressin or any other drug released by the device. This issue may adversely affect the performance of the device by delaying drug entry into the bloodstream, and if so, would have to be addressed for continued success of the device in enabling emergency therapy.

6.2.2. Short-Term Applications

Current protocols and requirements, if vasopressin were to be used in hemorrhagic shock, would require the establishment and maintenance of intravenous access for an infusion, which can be difficult in highly dynamic and chaotic conditions, such as those found on battlefields. Figure 6.1 shows an example of intravenous infusion implemented in an evacuation vehicle. An unexpected result obtained in this work was the finding that a subcutaneous injection of vasopressin was able to achieve sustained vasopressin levels, much like an intravenous infusion. This result opens new possibilities for the rapid delivery of vasopressin in emergency situations.

The first and simplest possibility is the direct subcutaneous injection of vasopressin by a medic on the battlefield following assessment of the hemorrhage. A device to inject drug solutions subcutaneously could be used for that purpose, or a simple syringe would suffice. The optimal location remains to be determined, but this solution could be implemented the fastest. Investigation of intramuscular injections of vasopressin may render the procedure even simpler if positive results are obtained. The use of subcutaneous vasopressin to address hemorrhagic shock is the object of a technology disclosure submitted to MIT's Technology Licensing Office.

The possibility of using subcutaneous injections also opens the doors for a more technological solution which does not require implantation. Figure 6.2 shows a conceptual render of such a solution, in the form of an armband to be worn by soldiers. The externalization of the device removes space and power limitations on the device, allowing all necessary components to be located on the armband with current technology. One or several spring-loaded syringes could be placed on it, along with control electronics, batteries and wireless antenna for remote activation by a medic. A rapid reconstitution device similar to the one demonstrated in this work in the syringe may also be implemented to allow for longer shelf life. The device would have to be ruggedized to withstand shocks, but could more easily be implemented than an implanted device, and would be more likely to be accepted by soldiers.

6.3. Figures

Figure 6.1: Wounded soldier in an evacuation vehicle with intravenous infusion bag.

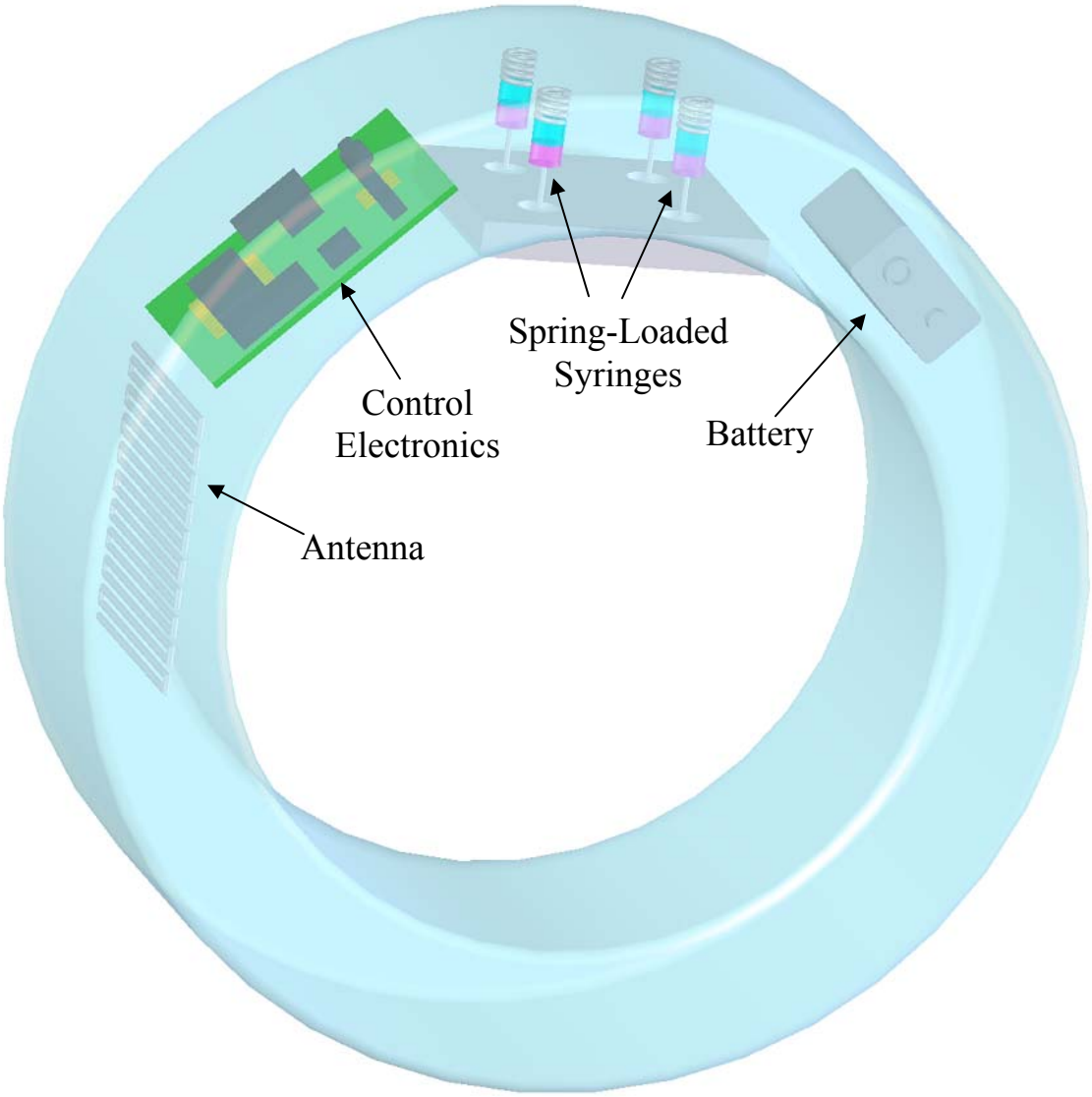

Figure 6.2: Conceptual render of an armband designed to inject vasopressin or other drugs subcutaneously in case of emergency. The armband would contain a number of spring-loaded syringes which can be activated to inject their load upon wireless triggering by a medic.